



Search for R-Parity Violating Decays of Supersymmetric Particles in e^+e^- Collisions at Centre-of-Mass Energies from 189 GeV to 202 GeV

R. Barate, D. Decamp, P. Ghez, C. Goy, S. Jezequel, J P. Lees, F. Martin, E. Merle, M.N. Minard, B. Pietrzyk, et al.

► To cite this version:

R. Barate, D. Decamp, P. Ghez, C. Goy, S. Jezequel, et al.. Search for R-Parity Violating Decays of Supersymmetric Particles in e^+e^- Collisions at Centre-of-Mass Energies from 189 GeV to 202 GeV. European Physical Journal C: Particles and Fields, 2001, 19, pp.415-428. in2p3-00007912

HAL Id: in2p3-00007912

<https://hal.in2p3.fr/in2p3-00007912>

Submitted on 15 May 2001

HAL is a multi-disciplinary open access archive for the deposit and dissemination of scientific research documents, whether they are published or not. The documents may come from teaching and research institutions in France or abroad, or from public or private research centers.

L'archive ouverte pluridisciplinaire **HAL**, est destinée au dépôt et à la diffusion de documents scientifiques de niveau recherche, publiés ou non, émanant des établissements d'enseignement et de recherche français ou étrangers, des laboratoires publics ou privés.

Search for R-Parity Violating Decays of Supersymmetric Particles in e^+e^- Collisions at Centre-of-Mass Energies from 189 GeV to 202 GeV

The ALEPH Collaboration¹

Abstract

Searches for the production of supersymmetric particles under the assumption that R-parity is violated via a single dominant $LL\bar{E}$, $LQ\bar{D}$ or $\bar{U}\bar{D}\bar{D}$ coupling were performed. These use the data collected by the ALEPH detector at LEP at centre-of-mass energies from 188.6 to 201.6 GeV. The numbers of candidate events observed in the data are consistent with Standard Model expectations. Upper limits on the production cross sections and lower limits on the masses of charginos, sleptons, squarks and sneutrinos are derived.

(Submitted to European Physical Journal C)

¹See next page for a list of the authors

The ALEPH Collaboration

R. Barate, D. Decamp, P. Ghez, C. Goy, S. Jezequel, J.-P. Lees, F. Martin, E. Merle, M.-N. Minard, B. Pietrzyk

Laboratoire de Physique des Particules (LAPP), IN²P³-CNRS, F-74019 Annecy-le-Vieux Cedex, France

S. Bravo, M.P. Casado, M. Chmeissani, J.M. Crespo, E. Fernandez, M. Fernandez-Bosman, Ll. Garrido,¹⁵ E. Graugés, J. Lopez, M. Martinez, G. Merino, R. Miquel, Ll.M. Mir, A. Pacheco, D. Paneque, H. Ruiz

Institut de Física d'Altes Energies, Universitat Autònoma de Barcelona, E-08193 Bellaterra (Barcelona), Spain⁷

A. Colaleo, D. Creanza, N. De Filippis, M. de Palma, G. Iaselli, G. Maggi, M. Maggi,¹ S. Nuzzo, A. Ranieri, G. Raso,²⁴ F. Ruggieri, G. Selvaggi, L. Silvestris, P. Tempesta, A. Tricomi,³ G. Zito

Dipartimento di Fisica, INFN Sezione di Bari, I-70126 Bari, Italy

X. Huang, J. Lin, Q. Ouyang, T. Wang, Y. Xie, R. Xu, S. Xue, J. Zhang, L. Zhang, W. Zhao

Institute of High Energy Physics, Academia Sinica, Beijing, The People's Republic of China⁸

D. Abbaneo, P. Azzurri, G. Boix,⁶ O. Buchmüller, M. Cattaneo, F. Cerutti, B. Clerbaux, G. Dissertori, H. Drevermann, R.W. Forty, M. Frank, F. Gianotti, T.C. Greening, J.B. Hansen, J. Harvey, D.E. Hutchcroft, P. Janot, B. Jost, M. Kado, V. Lemaitre, P. Maley, P. Mato, A. Minten, A. Moutoussi, F. Ranjard, L. Rolandi, D. Schlatter, M. Schmitt,²⁰ O. Schneider,² P. Spagnolo, W. Tejessy, F. Teubert, E. Tournefier,²⁶ A. Valassi, J.J. Ward, A.E. Wright

European Laboratory for Particle Physics (CERN), CH-1211 Geneva 23, Switzerland

Z. Ajaltouni, F. Badaud, S. Dessagne, A. Falvard, D. Fayolle, P. Gay, P. Henrard, J. Jousset, B. Michel, S. Monteil, J-C. Montret, D. Pallin, J.M. Pascolo, P. Perret, F. Podlyski

Laboratoire de Physique Corpusculaire, Université Blaise Pascal, IN²P³-CNRS, Clermont-Ferrand, F-63177 Aubière, France

J.D. Hansen, J.R. Hansen, P.H. Hansen, B.S. Nilsson, A. Wäänänen

Niels Bohr Institute, 2100 Copenhagen, DK-Denmark⁹

G. Daskalakis, A. Kyriakis, C. Markou, E. Simopoulou, A. Vayaki

Nuclear Research Center Demokritos (NRCD), GR-15310 Attiki, Greece

A. Blondel,¹² J.-C. Brient, F. Machefert, A. Rougé, M. Swynghedauw, R. Tanaka H. Videau

Laboratoire de Physique Nucléaire et des Hautes Energies, Ecole Polytechnique, IN²P³-CNRS, F-91128 Palaiseau Cedex, France

E. Focardi, G. Parrini, K. Zachariadou

Dipartimento di Fisica, Università di Firenze, INFN Sezione di Firenze, I-50125 Firenze, Italy

A. Antonelli, M. Antonelli, G. Bencivenni, G. Bologna,⁴ F. Bossi, P. Campana, G. Capon, V. Chiarella, P. Laurelli, G. Mannocchi,⁵ F. Murtas, G.P. Murtas, L. Passalacqua, M. Pepe-Altarelli²⁵

Laboratori Nazionali dell'INFN (LNF-INFN), I-00044 Frascati, Italy

M. Chalmers, A.W. Halley, J. Kennedy, J.G. Lynch, P. Negus, V. O'Shea, B. Raeven, D. Smith, P. Teixeira-Dias, A.S. Thompson

Department of Physics and Astronomy, University of Glasgow, Glasgow G12 8QQ, United Kingdom¹⁰

R. Cavanaugh, S. Dhamotharan, C. Geweniger, P. Hanke, V. Hepp, E.E. Kluge, G. Leibenguth, A. Putzer,

K. Tittel, S. Werner,¹⁹ M. Wunsch¹⁹

Kirchhoff-Institut für Physik, Universität Heidelberg, D-69120 Heidelberg, Germany¹⁶

R. Beuselinck, D.M. Binnie, W. Cameron, G. Davies, P.J. Dornan, M. Girone,¹ N. Marinelli, J. Nowell, H. Przysiezniak, J.K. Sedgbeer, J.C. Thompson,¹⁴ E. Thomson,²³ R. White

Department of Physics, Imperial College, London SW7 2BZ, United Kingdom¹⁰

V.M. Ghete, P. Girtler, E. Kneringer, D. Kuhn, G. Rudolph

Institut für Experimentalphysik, Universität Innsbruck, A-6020 Innsbruck, Austria¹⁸

E. Bouhova-Thacker, C.K. Bowdery, D.P. Clarke, G. Ellis, A.J. Finch, F. Foster, G. Hughes, R.W.L. Jones,¹ M.R. Pearson, N.A. Robertson, M. Smizanska

Department of Physics, University of Lancaster, Lancaster LA1 4YB, United Kingdom¹⁰

I. Giehl, F. Hölldorfer, K. Jakobs, K. Kleinknecht, M. Kröcker, A.-S. Müller, H.-A. Nürnberger, G. Quast,¹ B. Renk, E. Rohne, H.-G. Sander, S. Schmeling, H. Wachsmuth, C. Zeitnitz, T. Ziegler

Institut für Physik, Universität Mainz, D-55099 Mainz, Germany¹⁶

A. Bonissent, J. Carr, P. Coyle, C. Curtil, A. Ealet, D. Fouchez, O. Leroy, T. Kachelhoffer, P. Payre, D. Rousseau, A. Tilquin

Centre de Physique des Particules de Marseille, Univ Méditerranée, IN²P³-CNRS, F-13288 Marseille, France

M. Aleppo, S. Gilardoni, F. Ragusa

Dipartimento di Fisica, Università di Milano e INFN Sezione di Milano, I-20133 Milano, Italy.

A. David, H. Dietl, G. Ganis,²⁷ A. Heister, K. Hüttmann, G. Lütjens, C. Mannert, W. Männer, H.-G. Moser, S. Schael, R. Settles,¹ H. Stenzel, W. Wiedenmann, G. Wolf

Max-Planck-Institut für Physik, Werner-Heisenberg-Institut, D-80805 München, Germany¹⁶

J. Boucrot,¹ O. Callot, M. Davier, L. Duflot, J.-F. Grivaz, Ph. Heusse, A. Jacholkowska,¹ L. Serin, J.-J. Veillet, I. Videau, J.-B. de Vivie de Régie,²⁸ C. Yuan, D. Zerwas

Laboratoire de l'Accélérateur Linéaire, Université de Paris-Sud, IN²P³-CNRS, F-91898 Orsay Cedex, France

G. Bagliesi, T. Boccali, G. Calderini, V. Ciulli, L. Foà, A. Giammanco, A. Giassi, F. Ligabue, A. Messineo, F. Palla,¹ G. Sanguinetti, A. Sciabà, G. Sguazzoni, R. Tenchini,¹ A. Venturi, P.G. Verдини

Dipartimento di Fisica dell'Università, INFN Sezione di Pisa, e Scuola Normale Superiore, I-56010 Pisa, Italy

G.A. Blair, J. Coles, G. Cowan, M.G. Green, L.T. Jones, T. Medcalf, J.A. Strong, J.H. von Wimmersperg-Toeller

Department of Physics, Royal Holloway & Bedford New College, University of London, Surrey TW20 OEX, United Kingdom¹⁰

R.W. Clifft, T.R. Edgecock, P.R. Norton, I.R. Tomalin

Particle Physics Dept., Rutherford Appleton Laboratory, Chilton, Didcot, Oxon OX11 0QX, United Kingdom¹⁰

B. Bloch-Devaux,¹ D. Boumediene, P. Colas, B. Fabbro, E. Lançon, M.-C. Lemaire, E. Locci, P. Perez, J. Rander, J.-F. Renardy, A. Rosowsky, P. Seager,¹³ A. Trabelsi,²¹ B. Tuchming, B. Vallage

CEA, DAPNIA/Service de Physique des Particules, CE-Saclay, F-91191 Gif-sur-Yvette Cedex, France¹⁷

N. Konstantinidis, C. Loomis, A.M. Litke, G. Taylor

Institute for Particle Physics, University of California at Santa Cruz, Santa Cruz, CA 95064, USA²²

C.N. Booth, S. Cartwright, F. Combley, P.N. Hodgson, M. Lehto, L.F. Thompson

Department of Physics, University of Sheffield, Sheffield S3 7RH, United Kingdom¹⁰

K. Affholderbach, A. Böhrer, S. Brandt, C. Grupen, J. Hess, A. Misiejuk, G. Prange, U. Sieler

Fachbereich Physik, Universität Siegen, D-57068 Siegen, Germany¹⁶

C. Borean, G. Giannini, B. Gobbo

Dipartimento di Fisica, Università di Trieste e INFN Sezione di Trieste, I-34127 Trieste, Italy

H. He, J. Putz, J. Rothberg, S. Wasserbaech

Experimental Elementary Particle Physics, University of Washington, Seattle, WA 98195 U.S.A.

S.R. Armstrong, K. Cranmer, P. Elmer, D.P.S. Ferguson, Y. Gao, S. González, O.J. Hayes, H. Hu, S. Jin, J. Kile, P.A. McNamara III, J. Nielsen, W. Orejudos, Y.B. Pan, Y. Saadi, I.J. Scott, J. Walsh, J. Wu, Sau Lan Wu, X. Wu, G. Zobernig

Department of Physics, University of Wisconsin, Madison, WI 53706, USA¹¹

¹Also at CERN, 1211 Geneva 23, Switzerland.

²Now at Université de Lausanne, 1015 Lausanne, Switzerland.

³Also at Dipartimento di Fisica di Catania and INFN Sezione di Catania, 95129 Catania, Italy.

⁴Deceased.

⁵Also Istituto di Cosmo-Geofisica del C.N.R., Torino, Italy.

⁶Supported by the Commission of the European Communities, contract ERBFMBICT982894.

⁷Supported by CICYT, Spain.

⁸Supported by the National Science Foundation of China.

⁹Supported by the Danish Natural Science Research Council.

¹⁰Supported by the UK Particle Physics and Astronomy Research Council.

¹¹Supported by the US Department of Energy, grant DE-FG0295-ER40896.

¹²Now at Département de Physique Corpusculaire, Université de Genève, 1211 Genève 4, Switzerland.

¹³Supported by the Commission of the European Communities, contract ERBFMBICT982874.

¹⁴Also at Rutherford Appleton Laboratory, Chilton, Didcot, UK.

¹⁵Permanent address: Universitat de Barcelona, 08208 Barcelona, Spain.

¹⁶Supported by the Bundesministerium für Bildung, Wissenschaft, Forschung und Technologie, Germany.

¹⁷Supported by the Direction des Sciences de la Matière, C.E.A.

¹⁸Supported by the Austrian Ministry for Science and Transport.

¹⁹Now at SAP AG, 69185 Walldorf, Germany

²⁰Now at Harvard University, Cambridge, MA 02138, U.S.A.

²¹Now at Département de Physique, Faculté des Sciences de Tunis, 1060 Le Belvédère, Tunisia.

²²Supported by the US Department of Energy, grant DE-FG03-92ER40689.

²³Now at Department of Physics, Ohio State University, Columbus, OH 43210-1106, U.S.A.

²⁴Also at Dipartimento di Fisica e Tecnologia Relative, Università di Palermo, Palermo, Italy.

²⁵Now at CERN, 1211 Geneva 23, Switzerland.

²⁶Now at ISN, Institut des Sciences Nucléaires, 53 Av. des Martyrs, 38026 Grenoble, France.

²⁷Now at Università degli Studi di Roma Tor Vergata, Dipartimento di Fisica, 00133 Roma, Italy.

²⁸Now at Centre de Physique des Particules de Marseille, Univ Méditerranée, F-13288 Marseille, France.

1 Introduction

Minimal supersymmetric extensions of the Standard Model (MSSM) [1] usually make the assumption that R-parity, $R_p = -1^{3B+L+2S}$, is conserved [2], where B denotes the baryon number, L the lepton number and S the spin of a field. The conservation of R-parity is not required theoretically and models in which R-parity is violated can be constructed which are compatible with existing experimental constraints.

The R-parity violating terms of the superpotential considered here are [3]

$$W_{R_p} = \lambda_{ijk} L_i L_j \bar{E}_k + \lambda'_{ijk} L_i Q_j \bar{D}_k + \lambda''_{ijk} \bar{U}_i \bar{D}_j \bar{D}_k, \quad (1)$$

where \bar{D}, \bar{U} (\bar{E}) are the down-like and up-like quark (lepton) singlet superfields, and Q (L) is the quark (lepton) doublet superfield respectively; λ, λ' and λ'' are Yukawa couplings and $i, j, k = 1, 2, 3$ are generation indices. The presence of such R-parity violating terms imply that the lightest supersymmetric particle (LSP) is no longer stable and that sparticles can be produced singly. The sparticle decays which proceed directly to standard model particles are called *direct* decays. Decays in which the sparticle first decays, conserving R-parity, to the lightest neutralino are referred to as *indirect* decays. Both cases are illustrated in Fig. 1. Other cascade decays are possible but not considered in the following.

In this paper a new search for the resonant production of single sneutrinos decaying indirectly is presented. In addition, previously reported searches for both direct and indirect decays of pair produced sparticles at 183 GeV [4] are extended and applied to new data at higher energies. In particular, new selections for indirect decays of sleptons and squarks via the $LQ\bar{D}$ operator are developed. Table 1 summarises the possible decays and indicates those addressed in this paper. Other collaborations at LEP have published similar searches at lower energies [5, 6, 7, 8, 9].

The following assumptions are made throughout:

- All three terms in Equation (1) are addressed, however only one term for a specific set of indices (i, j and k) is considered non zero. Unless otherwise stated the derived limits correspond to the choice of indices for the coupling giving the worst limit.
- The lifetime of the particles can be neglected, i.e. the mean flight path is less than 1 cm.
- Results are interpreted within the framework of the MSSM. Gaugino mass unification at the electroweak scale is assumed, giving the condition $M_1 = \frac{5}{3}M_2 \tan^2 \theta_W$.
- For the case of the charginos and neutralinos, only large values of the universal scalar mass m_0 are considered; this implies the *direct* decays of the lightest chargino and the next-to-lightest neutralino are suppressed. It also implies three-body decay kinematics for the lightest neutralino.

Table 1: For each sparticle the table lists whether the decay mode is searched for (\bullet), possible but not considered (\diamond), or not possible (\times). Those processes marked with \dagger were not considered in the 183 GeV results [4].

	$LL\bar{E}$		$LQ\bar{D}$		$\bar{U}\bar{D}\bar{D}$	
	Direct	Indirect	Direct	Indirect	Direct	Indirect
χ^\pm	\diamond	\bullet	\diamond	\bullet	\diamond	\bullet
χ'	\diamond	\bullet	\diamond	\bullet	\diamond	\bullet
$\tilde{e}, \tilde{\mu}, \tilde{\tau}$	\bullet	\bullet	$\bullet(\tilde{I}_L)$	\bullet^\dagger	\times	\bullet
$\tilde{\nu}_e, \tilde{\nu}_\mu, \tilde{\nu}_\tau$	\bullet	\bullet	\bullet	\bullet^\dagger	\times	\bullet
\tilde{u}	\times	\bullet	\bullet	\bullet^\dagger	$\bullet(\tilde{u}_R)$	\bullet
\tilde{d}	\times	\bullet	\bullet	\bullet^\dagger	$\bullet(\tilde{d}_R)$	\bullet

The search results reported here use data collected by the ALEPH detector in 1998 and 1999 from e^+e^- collisions at centre-of-mass energies between 188.6 GeV and 201.6 GeV. The total data sample used corresponds to an integrated recorded luminosity of 173.6 pb^{-1} at 188.6 GeV, 29.0 pb^{-1} at 191.6 GeV, 80.1 pb^{-1} at 195.5 GeV, 85.9 pb^{-1} at 199.5 GeV and 41.9 pb^{-1} at 201.6 GeV.

This paper is organised as follows: after a brief description of the ALEPH detector in Section 2, the Monte Carlo samples used for signal and background generation are detailed in Section 3. Sections 4, 5 and 6 give the results and interpretations for each of the R-parity violating couplings, and finally Section 7 gives a summary of the results.

2 The ALEPH Detector

The ALEPH detector is described in detail in Ref. [10]. An account of the performance of the detector and a description of the standard analysis algorithms can be found in Ref. [11]. Here, only a brief description of the detector components and the algorithms relevant for this analysis is given.

The trajectories of charged particles are measured with a silicon vertex detector, a cylindrical drift chamber, and a large time projection chamber (TPC). The central detectors are immersed in a 1.5 T axial magnetic field provided by a superconducting solenoidal coil. The electromagnetic calorimeter (ECAL), placed between the TPC and the coil, is a highly segmented sampling calorimeter which is used to identify electrons and photons and to measure their energies. The luminosity monitors extend the calorimetric coverage down to 34 mrad from the beam axis. The hadron calorimeter (HCAL) consists of the iron return yoke of the magnet instrumented with streamer tubes. It provides a measurement of hadronic energy and, together with the external muon chambers, muon identification. The calorimetric and tracking information are combined in an energy flow algorithm which

gives a measure of the total energy, and therefore the missing energy, with an uncertainty of $(0.6\sqrt{E} + 0.6)$ GeV.

Electron identification is primarily based upon the matching between the measured momentum of the charged track and the energy deposited in the ECAL. Additional information from the shower profile in the ECAL and the measured rate of specific ionisation energy loss in the TPC are also used. Muons are separated from hadrons by their characteristic pattern in HCAL and the presence of associated hits in the muon chambers.

3 Monte Carlo Samples and Efficiencies

The signal topologies were simulated using the **SUSYGEN** Monte Carlo program [12] modified as described in Ref. [4]. The events were subsequently passed through either a full simulation or a faster simplified simulation of the ALEPH detector. Where the fast simulation was used a subselection of these were also passed through the full simulation to verify the accuracy of the fast simulation.

Samples of all major backgrounds were generated and passed through the full simulation, corresponding to at least 10 times the collected luminosity in the data. The **PYTHIA** generator [13] was used to produce $q\bar{q}$ events and four-fermion final states from $W\nu$, ZZ and Zee , with a vector-boson invariant mass cut of $0.2 \text{ GeV}/c^2$ for ZZ and $W\nu$, and $2 \text{ GeV}/c^2$ for Zee . Pairs of W bosons were generated with **KORALW** [14]. The **KORALW** cross sections were adjusted to agree with the most recent theoretical calculations [15]. Pair production of leptons was simulated with **UNIBAB** [16] (electrons) and **KORALZ** [17] (muons and taus). The $\gamma\gamma \rightarrow f\bar{f}$ processes were generated with **PHOT02** [18].

The selections were optimised to give the minimum expected 95% C.L. excluded cross section in the absence of a signal for masses close to the high end of the expected sensitivity. Selection efficiencies were determined as a function of the SUSY particle masses and the generation structure of the R-parity violating couplings λ_{ijk} , λ'_{ijk} and λ''_{ijk} .

The cross section limits were evaluated at the highest centre-of-mass energy. Where data taken at a range of centre-of-mass energies contributed to the exclusions the data were weighted with the expected evolution of the cross-section with \sqrt{s} .

The systematic uncertainties on the selection efficiencies are of order of 4–5% and are dominated by the statistical uncertainty of the Monte Carlo signal samples, with small additional contributions from lepton identification and energy flow reconstruction. They were taken into account by reducing the selection efficiencies by one standard deviation of the statistical error.

When setting the limits, background subtraction was performed for two- and four-fermion final states according to the prescription given in Ref. [19]. To take into account the uncertainties on the background estimates, the amount of background subtracted is reduced. For two-fermion processes it was reduced by its statistical error. The contribution from WW and ZZ processes were reduced by the statistical error added in quadrature with

1% of its estimate. The components from $W e \nu$ and Zee processes were reduced by 20% of their estimate. No background is subtracted for the $\gamma\gamma \rightarrow f\bar{f}$ processes.

4 Decays via a dominant $LL\bar{E}$ coupling

Under the assumption of a dominant $LL\bar{E}$ coupling, the decay topologies can consist of as little as two acoplanar leptons in the simplest case (direct slepton decay or single resonant sneutrino production), or they may consist of as many as six leptons plus four neutrinos in the most complicated case (indirect chargino decay). In addition to the purely leptonic topologies, the MSSM cascade decays of charginos into lighter neutralinos may produce multi-jet and multi-lepton final states. No direct decays are possible for the squarks.

The absolute lower limit on the mass of the lightest neutralino of $23 \text{ GeV}/c^2$ obtained in Ref. [20], which is valid for any choice of μ , M_2 , m_0 and generational indices (i , j and k), is used to restrict the range of neutralino mass considered for the indirect decays.

The various selections addressing the above topologies, the expected backgrounds, and the numbers of candidates selected in the data at $\sqrt{s} = 188.6\text{--}201.6 \text{ GeV}$ are summarised in Table 2. Details of the “6 Leptons + \cancel{E} ”, the “4 Leptons + \cancel{E} ” and the “4 Leptons” analyses are given in Ref. [20]. The “Acoplanar Leptons” and “Leptons and Hadrons” selections are described in Ref. [4], although the “Leptons and Hadrons” has been updated for the increased centre-of-mass energy as described in section 4.2. Wherever the “Acoplanar Leptons” selection is used the expected combination of final state flavours (e, μ and τ) for each process is used to set the exclusion.

4.1 Single resonant sneutrino production

Single resonant production of sneutrinos [21] can occur for the specific couplings λ_{121} and λ_{131} . The sneutrino may decay indirectly through the diagram shown in Fig. 2 or directly to e^+e^- . Since the production cross-section is a function of $|\lambda_{1j1}|^2$, limits can be set on the magnitude of λ_{1j1} as a function of the sneutrino mass. The best sensitivity is obtained for the case where the sneutrino is produced exactly on shell, $\sqrt{s} = M_{\tilde{\nu}}$. For centre-of-mass energies above $M_{\tilde{\nu}}$ initial state radiation from the e^+e^- system allows a radiative return to the sneutrino resonance. There is also some sensitivity for $M_{\tilde{\nu}} > \sqrt{s}$ via the production of a virtual sneutrino.

Since the final state consists of two leptons and two neutrinos the “Acoplanar Leptons” selection is used to select these events. Figure 3 shows the excluded values of λ_{121} and λ_{131} as a function of the mass of the sneutrinos; all data taken in the range $\sqrt{s} = 130$ to 189 GeV are used. The data and background numbers for the lower energies are given in Ref. [4, 20]. Also shown are the results for the direct decays from electroweak fits [22] and the exclusion from low energy measurements [23].

Table 2: The observed numbers of events in the data and the corresponding Standard Model background expectations for the $LL\bar{E}$ selections.

\sqrt{s} (GeV)	188.6		191.6		195.5		199.5		201.6		All	
Selection	Data	SM	Data	SM	Data	SM	Data	SM	Data	SM	Data	SM
Leptons and Hadrons	10	7.8	1	1.4	4	4.0	5	4.5	0	2.1	20	20
6 Leptons + \cancel{E}	2	1.0	1	0.2	0	0.4	0	0.5	0	0.2	3	2.2
4 Leptons + \cancel{E}	4	4.6	1	0.8	1	2.0	4	2.8	1	1.7	11	12
$llll$	3	5.1	1	0.7	3	1.7	8	2.3	0	1.3	15	11
$ll\tau\tau$	2	2.0	0	0.3	2	0.9	0	0.9	0	0.4	4	4.6
$\tau\tau\tau\tau$	5	4.2	1	0.7	1	1.9	5	2.1	0	1.1	12	10
Acoplanar Leptons	192	211	22	34	93	87	100	94	41	45	448	471

4.2 Charginos and neutralinos decaying via $LL\bar{E}$

Depending on the masses of the gauginos and on the lepton flavour composition in the decay, the indirect decays of charginos to neutralinos and of heavier neutralinos to lighter neutralinos populate different regions in track multiplicity, visible mass and leptonic energy. For this reason three different subselections were developed [4], covering topologies with large leptonic energies and at least two jets (Subselection I), topologies with small multiplicities and large leptonic energy fractions (Subselection II), and topologies with a moderate leptonic energy fraction (Subselection III). The combination of the three subselections is defined as the “Leptons and Hadrons” selection. The complete set of cuts, updated for $\sqrt{s} > 184$ GeV is shown in Table 3.

Interpreting the results, shown in Table 2, in the framework of the MSSM, 95% C.L. exclusion limits are derived in the (μ, M_2) plane and shown in Fig. 4(a) for large scalar masses $m_0 = 500$ GeV/ c^2 . The corresponding lower limit on the mass of the lightest chargino is essentially at the kinematic limit for pair production.

The searches for the lightest and second lightest neutralino do not extend the excluded region in the (μ, M_2) plane beyond that achieved with the chargino search alone.

Table 3: The list of cuts for the “Leptons and Hadrons” selection, which is used for charginos and squarks decaying indirectly via the $LL\bar{E}$ operator. The event variables are defined in Ref. [4].

Subselection I	Subselection II	Subselection III
$N_{\text{ch}} \geq 5$ $M_{\text{vis}} > 25 \text{ GeV}/c^2$	$5 \leq N_{\text{ch}} \leq 15$ $20 \text{ GeV}/c^2 < M_{\text{vis}} < 75\%\sqrt{s}$	$N_{\text{ch}} \geq 11$ $55\%\sqrt{s} < M_{\text{vis}} < 80\%\sqrt{s}$
$p_{\perp}^{\text{miss}} > 3.5\%\sqrt{s}$ $ p_z^{\text{miss}} < 20 \text{ GeV}/c$	$p_{\perp}^{\text{miss}} > 2.5\%\sqrt{s}$	$p_{\perp}^{\text{miss}} > 5\%\sqrt{s}$ $N_{\text{ch}}^{\text{jet}} \geq 1$
$y_5 > 0.006$	$y_3 > 0.009$ $y_4 > 0.0026$	$y_3 > 0.025$ $y_4 > 0.012$ $y_5 > 0.004$ $T < 0.85$
$N_{\text{lep}} \geq 1$ $E_{\text{nonlep}} < 50\%\sqrt{s}$ $E_{\text{had}} < 28\%E_{\text{vis}}$	$N_{\text{lep}} \geq 1$ $E_{\text{nonlep}} < 50\%\sqrt{s}$ $E_{\text{had}} < 22\%E_{\text{lep}}$	$N_{\text{lep}} \geq 1$ $E_{\text{lep}} > 20\%E_{\text{had}}$
$\chi_{\text{WW}}^2 > 3.8$		

4.3 Squarks decaying via $LL\bar{E}$

Although squarks cannot decay directly with an $LL\bar{E}$ coupling, they may decay indirectly to the lightest neutralino. This topology is searched for by means of the “Leptons and Hadrons” selection. The 95% C.L. squark mass limits are presented as functions of M_{χ} in Fig. 5 for the case of \tilde{t}_1 and \tilde{b}_1 squarks. The following limits upon the right-handed squarks can be derived: $M_{\tilde{u}_R} > 90 \text{ GeV}/c^2$ and $M_{\tilde{d}_R} > 89 \text{ GeV}/c^2$ for any λ_{ijk} .

4.4 Sleptons decaying via $LL\bar{E}$

A right-handed slepton can decay directly via the $LL\bar{E}$ coupling to a lepton and anti-neutrino, hence the acoplanar lepton selection is used. For a given choice of generation indices the decay will produce two final states equally; for the coupling λ_{ijk} these decays are $\tilde{l}_R^k \rightarrow l^i \bar{\nu}_{lj}$ or $\bar{\nu}_{li} l^j$. Excluded cross sections are shown in Fig. 6(a) for the different mixtures of acoplanar lepton states. The MSSM production cross section for right-handed smuon pairs and selectron pairs at $\mu = -200 \text{ GeV}/c^2$ and $\tan\beta = 2$ are superimposed. The cross section limit translates into a lower bound on the smuon (or stau) mass of $M_{\tilde{\mu}_R, \tilde{\tau}_R} > 81 \text{ GeV}/c^2$ and $M_{\tilde{e}_R} > 92 \text{ GeV}/c^2$ ($\mu = -200 \text{ GeV}/c^2$, $\tan\beta = 2$) for the direct decays and the worst case coupling.

Indirect decays of sleptons are selected using the “Six Leptons + \cancel{E} ” selection. Limits corresponding to this case are shown in Fig. 6(b), (c), and (d). Using the bound of $M_{\chi} > 23 \text{ GeV}/c^2$ these limits can be interpreted as the mass limits $M_{\tilde{e}_R} > 93 \text{ GeV}/c^2$ ($\mu = -200 \text{ GeV}/c^2$, $\tan\beta = 2$), $M_{\tilde{\mu}_R} > 92 \text{ GeV}/c^2$ and $M_{\tilde{\tau}_R} > 91 \text{ GeV}/c^2$ for the worst

case coupling.

4.5 Sneutrinos decaying via $LL\bar{E}$

In pair production each sneutrino can decay directly into pairs of charged leptons giving the final states $eeee$, $ee\mu\mu$, $ee\tau\tau$, $\mu\mu\mu\mu$, $\mu\mu\tau\tau$ and $\tau\tau\tau\tau$. The different final states correspond to different choices of generation indices. The “Four Lepton” selection was used to derive exclusion limits on the sneutrino pair production cross section shown in Fig. 7(a). These limits translate into a lower bound on the electron sneutrino mass of $M_{\tilde{\nu}_e} > 98 \text{ GeV}/c^2$ ($\mu = -200 \text{ GeV}/c^2$, $\tan\beta = 2$) and the muon sneutrino mass of $M_{\tilde{\nu}_\mu} > 86 \text{ GeV}/c^2$ for direct decays and the worst case coupling.

Indirect decays of sneutrinos are selected using the “Four Leptons + \cancel{E} ” selection. The limits in the $(M_\chi, M_{\tilde{\nu}})$ plane corresponding to this case are shown in Fig. 7(b) and (c). Using the bound $M_\chi > 23 \text{ GeV}/c^2$ this limit can be interpreted as $M_{\tilde{\nu}_{\mu,\tau}} > 83 \text{ GeV}/c^2$ and $M_{\tilde{\nu}_e} > 94 \text{ GeV}/c^2$ for the worst case coupling, where the cross section for the electron sneutrino is evaluated at $\mu = -200 \text{ GeV}/c^2$ and $\tan\beta = 2$.

5 Decays via a dominant $LQ\bar{D}$ Coupling

For a dominant $LQ\bar{D}$ operator the event topologies are mainly characterised by large hadronic activity, possibly with some leptons and/or missing energy. In the simplest case the topology consists of four-jet final states, and in more complicated scenarios of multi-jet and multi-lepton and/or multi-neutrino states. A summary of the results of the various selections is given in Table 4.

The acoplanar jet selection (AJ-H) and the four jets and missing energy selection (4JH) developed for R-parity conserving SUSY searches are used [24]. The “MultiJets + Leptons” and the “2J+2 τ ” selections are updated from Ref. [4] and reoptimised for the higher centre-of-mass energy as described below. The “Jets-HM” selection is a retuned version of the “MultiJets + Leptons” subselection I for a high visible mass system. The “4 Jets + 2 τ ” is unchanged from Ref. [25]. Two new selections for five jets and one isolated lepton and four jets and two isolated leptons, “5 Jets + 1 Iso. l ” and “4 Jets + 2 Iso. l ”, are described below.

5.1 Charginos and neutralinos decaying via $LQ\bar{D}$

Three subselections were developed to select the chargino indirect topologies [4]; some cuts have been reoptimised for the higher centre-of-mass energy. Subselection I is designed to select final states based on hadronic activity, e.g. $\chi^+\chi^- \rightarrow qq\bar{q}\bar{q}\chi\chi$; subselection II is designed for decays such as $\chi^+\chi^- \rightarrow l\nu qq\chi\chi$ where the leptonic energy is larger, and subselection III is designed to select the decays $\chi^+\chi^- \rightarrow l\nu l\nu\chi\chi$. The combination of the

Table 4: The observed numbers of events in the data and the Standard Model background expectations for the $LQ\bar{D}$ selections.

\sqrt{s} (GeV)	188.6		191.6		195.5		199.5		201.6		All	
Selection	Data	SM	Data	SM	Data	SM	Data	SM	Data	SM	Data	SM
MultiJets + Leptons	13	11	1	1.8	6	4.7	3	5.2	5	2.6	28	26
Jets-HM	11	8.7	1	1.3	3	3.1	1	2.8	3	1.3	19	17
4 Jets + 2τ	10	13	2	2.0	1	5.1	7	5.3	5	2.7	25	28
Four-Jets	684	754	143	127	322	351	336	370	147	179	1632	1780
2 Jets + 2τ	10	11	1	1.9	5	5.8	6	5.2	3	2.5	25	26
AJ-H	10	12	2	2.2	9	6.8	7	8.6	10	4.6	38	34
4JH	5	7.8	1	1.3	3	3.7	0	3.9	4	2.0	13	19
5 Jets + 1 Iso. l	4	4.2	1	0.7	1	1.9	0	1.9	0	0.9	6	9.6
4 Jets + 2 Iso. l	0	3.1	0	0.5	1	1.3	3	1.5	1	0.7	5	7.1

Table 5: The list of cuts for the “Multi-jets plus Leptons” selection used to select indirect chargino decays via the $LQ\bar{D}$ operator. The “Jets-HM” selection is also listed; this is used to select intermediate ΔM indirect squark decays with high visible mass. Primed event variables are calculated from physical quantities excluding identified leptons. The event variables are defined in Ref. [4].

Subselection I	Subselection II	Subselection III	Jets-HM
$N_{\text{ch}} \geq 10$ $M_{\text{vis}} > 45 \text{ GeV}/c^2$ $\Theta_{\text{miss}} > 30^\circ$			$N_{\text{ch}} \geq 30$ $M_{\text{vis}} > 100 \text{ GeV}/c^2$ $\Theta_{\text{miss}} > 30^\circ$
$M'_{\text{vis}} > 50\%\sqrt{s}$ $T < 0.9$ $y_5 > 0.003$ $y_6 > 0.002$ $E_T > 80 \text{ GeV}$	$M'_{\text{vis}} < 50\%\sqrt{s}$ $T < 0.74$ $y'_4 > 0.0047$ $\left(\begin{array}{c} \Phi'_{\text{aco}} < 145^\circ \\ \text{or} \\ y_6 > 0.002 \end{array} \right)$	$M'_{\text{vis}} < 65 \text{ GeV}/c^2$ $T < 0.8$ $y'_4 > 0.001$ $y_6 > 0.00035$	$M'_{\text{vis}} > 50\%\sqrt{s}$ $T < 0.85$ $y_5 > 0.003$ $y_6 > 0.002$ $E_T > 80 \text{ GeV}$
$E_{\text{jet}}^{\text{em}} < 90\%E_{\text{jet}}$ $E_{10}^{\text{iso}} < 5 \text{ GeV}$	$E_{\text{lep}} < 40 \text{ GeV}$ $E_{\text{had}} < 2.5E_{\text{lep}}$	$E_{\text{had}} < 47\%E_{\text{lep}}$	$E_{\text{jet}}^{\text{em}} < 85\%E_{\text{jet}}$ $E_{10}^{\text{iso}} < 5 \text{ GeV}$
$[0.55(M'_{\text{vis}} - 120) + \Phi'_{\text{aco}}] < 180^\circ$	$\chi_{\text{WW}}^2 > 3.8$		$[0.55(M'_{\text{vis}} - 120) + \Phi'_{\text{aco}}] < 190^\circ$

three subselections is defined as the “Multi-jets plus Leptons” selection. The complete set of cuts is shown in Table 5.

Interpreting these results in the framework of the MSSM, 95% C.L. exclusion limits are derived in the (μ, M_2) plane and shown in Fig. 4(b) for large scalar masses ($m_0 = 500 \text{ GeV}/c^2$). The corresponding lower limit on the mass of the lightest chargino is essentially at the kinematic limit for pair production.

The searches for the lightest and second lightest neutralino do not extend the excluded region in the (μ, M_2) plane beyond that achieved with the chargino search alone.

5.2 Squarks decaying via $LQ\bar{D}$

A squark can decay directly to a quark and either a lepton or a neutrino leading to topologies with acoplanar jets and up to two leptons. Couplings with electrons or muons in the final state are not considered as existing limits from the Tevatron [26] exclude the possibility of seeing such a signal at LEP. To select $\tilde{q} \rightarrow q\tau$ and $\tilde{q} \rightarrow q\nu$, the “2J+2 τ ” and the “AJ-H” selections are used. The “2J+2 τ ” selection is unchanged from Ref. [4] except that the sliding mass window is now $10 \text{ GeV}/c^2$ wide centred on the squark mass. Examples of limits for squark production are shown in Fig. 8. In particular, for a dominant λ'_{33k} coupling, which implies $\text{Br}(\tilde{t}_L \rightarrow q\tau) = 100\%$, a lower limit of $93 \text{ GeV}/c^2$ is obtained for $M_{\tilde{t}_L}$.

Table 6: The list of cuts for the “5 Jets + 1 Isolated Leptons” and “4 Jets + 2 Isolated Leptons” selections, as used for the indirect squark and slepton searches decaying via an $LQ\bar{D}$ operator. M''_{vis} is the visible mass after the two leading leptons are removed. Other variables are defined in Ref. [4].

5 Jets + 1 Iso. l	4 Jets + 2 Iso. l
$N_{\text{ch}} > 9$ $E_{\text{vis}} < 95\%\sqrt{s}$ $N_{\text{lep}} \geq 1$ $p_{\perp}^{\text{miss}} > 5 \text{ GeV}/c$ $\Theta_{\text{miss}} > 18^\circ$	$N_{\text{ch}} > 9$ $E_{\text{vis}} > 65\%\sqrt{s}$ $N_{\text{lep}} \geq 2$ (same flavour e or μ)
$E_{l_1} > 10 \text{ GeV}$ $E_{l_1}^{\text{iso}} < 5 \text{ GeV}$	$E_{l_1} > 5 \text{ GeV}, E_{l_2} > 5 \text{ GeV}$ $E_{l_1}^{\text{iso}} < 5 \text{ GeV}, E_{l_2}^{\text{iso}} < 5 \text{ GeV}$
$y_5 > 0.003$ $y_6 > 0.001$	$y_5 > 0.001$ $y_6 > 0.0005$
$\min \{ M_{\text{vis}} - 91.2 , M''_{\text{vis}} - 91.2 \} > 3 \text{ GeV}/c^2$	$ M''_{\text{vis}} - 91.2 > 5 \text{ GeV}/c^2$
$\chi^2_{\text{WW}} > 3.8$	

Indirect decays of squarks via the $LQ\bar{D}$ operator will give six jets and up to two charged leptons. These are selected by the “4 Jets + 2τ ” selection if $M_\chi \leq 20 \text{ GeV}/c^2$, either the “5 Jets + 1 Iso. l ” or “Multi-jets plus Leptons” if $(M_{\tilde{q}} - M_\chi) \leq 15 \text{ GeV}/c^2$, otherwise the “Jets-HM” selection is used. The cuts used for the “5 Jets + 1 Iso. l ” selection are listed in Table 6. Limits for the optimistic case of left-handed squarks are shown in Fig. 9. The following limits for \tilde{t}_L and \tilde{b}_L are derived: $M_{\tilde{t}_L} > 84 \text{ GeV}/c^2$ and $M_{\tilde{b}_L} > 74 \text{ GeV}/c^2$.

5.3 Sleptons and sneutrinos decaying via $LQ\bar{D}$

Direct decays of sleptons and sneutrinos via the $LQ\bar{D}$ operator lead to four jet final states. The “Four-Jets” selection from Ref. [4] is applied. The distributions of the di-jet masses for data and Monte Carlo are shown in Fig. 10(a). Fewer events are observed around the W mass peak region than expected. Limits are derived by sliding a mass window of $5 \text{ GeV}/c^2$ across the di-jet mass distribution. The results are shown in Fig. 10(b) and imply $M_{\tilde{\nu}_\mu} > 77 \text{ GeV}/c^2$ and $M_{\tilde{\mu}_L} > 79 \text{ GeV}/c^2$.

Indirect decays of the sleptons via the $LQ\bar{D}$ operator will give two, three or four leptons and four jets in the final state; two leptons will be of the same flavour as the initial sleptons. The indirect decays of sneutrinos will give a final state with four jets, up to two leptons and missing energy. For selectrons and smuons the “4 Jets + 2 Iso. l ” selection is used except for the special case of $\lambda'_{3jk} \neq 0$ and $(M_{\tilde{l}_R} - M_\chi) < 10 \text{ GeV}/c^2$ where the “4 Jets + 2τ ” selection is used. The cuts used in the “4 Jets + 2 Iso. l ” are listed in Table 6. Indirect stau decays are selected with the “5 Jets + 1 Iso. l ” selection if $M_\chi > 20 \text{ GeV}/c^2$.

Table 7: The list of cuts for the “Four Jets + \cancel{E} ” and “Many Jets + \cancel{E} ” selections, as used for the indirect sneutrino searches via a $\bar{U}\bar{D}\bar{D}$ operator.

Four Jets + \cancel{E}	Many Jets + \cancel{E}
$N_{\text{ch}} > 8$ $ p_z^{\text{miss}} /p^{\text{miss}} < 0.95$ $E_{\text{jet}}^{\text{em}} < 95\% E_{\text{jet}}, E_T > 60 \text{ GeV}, E_{\text{lep}} < 15 \text{ GeV}$	
$0.25 < E_{\text{vis}}/\sqrt{s} < 0.75$ $\Delta\phi_T < 170^\circ$ $0.5 < T < 0.97$	$0.5 < E_{\text{vis}}/\sqrt{s} < 0.95$ $0.6 < T < 0.97$
$y_4 > 0.001$ $y_6 > 0.0003$	$y_4 > 0.005$ $y_6 > 0.002 \text{ (} 0.005 \text{ if } M_\chi > 60 \text{ GeV)}$
$ M_{12-34} < 10 \text{ GeV}/c^2$ $ M_{12+34} - 2M_\chi < M_\chi/3$	if $M_\chi < 60 \text{ GeV}/c^2$: $ M_{12-34} < 10 \text{ GeV}/c^2$ if $M_\chi < 60 \text{ GeV}/c^2$: $ M_{12+34} - 2M_\chi < M_\chi/3$

and either $\lambda'_{2jk} \neq 0$ or $\lambda'_{1jk} \neq 0$, otherwise the inclusive combination of the “5 Jets + 1 Iso. l ” and the “Leptons and Hadrons” selections is used. The sneutrinos are selected with the “4JH” selection for $M_\chi > 20 \text{ GeV}/c^2$ and “AJ-H” (acoplanar jets) otherwise. Limits for these decays are shown in Fig. 11 and Fig. 12. The limits are $M_{\tilde{e}_R} > 89 \text{ GeV}/c^2$, $M_{\tilde{\mu}_R} > 86 \text{ GeV}/c^2$, $M_{\tilde{\tau}_R} > 73 \text{ GeV}/c^2$, $M_{\tilde{\nu}_e} > 89 \text{ GeV}/c^2$ and $M_{\tilde{\nu}_\mu} > 75 \text{ GeV}/c^2$ for the worst case couplings; the selectron and electron sneutrino cross sections are evaluated at $\mu = -200 \text{ GeV}/c^2$ and $\tan\beta = 2$.

6 Decays via a dominant $\bar{U}\bar{D}\bar{D}$ coupling

For a dominant $\bar{U}\bar{D}\bar{D}$ operator the final states are characterised by topologies having many hadronic jets, possibly associated with leptons and missing energy. A number of selections are used: “Four Jets”, “Four Jets-Broad”, “Many Jets”, “Many Jets + Leptons”, “Four Jets + 2 Leptons”, “Many Jets + 2 Leptons”, “Four Jets + \cancel{E} ” and “Many Jets + \cancel{E} ”, all introduced in Ref. [4]. The latter two selections, which require missing energy, have been slightly modified for the higher energy and are summarised in Table 7. These selections rely mainly on two characteristics of the events: mass reconstruction of the pair produced sparticles and/or the presence of many jets in the event. Table 8 gives a list of all the selections and the numbers of observed and expected events.

6.1 Charginos and neutralinos decaying via $\bar{U}\bar{D}\bar{D}$

The decay of the lightest neutralino and direct decays of the chargino both lead to six hadronic jets in the final state. The indirect chargino decays give rise to a variety of final

Table 8: The observed numbers of events in the data and the corresponding Standard Model background expectations for the $\bar{U}\bar{D}\bar{D}$ selections, quoted with any sliding mass cuts removed.

\sqrt{s} (GeV)	188.6		191.6		195.5		199.5		201.6		All	
Selection	Data	SM	Data	SM	Data	SM	Data	SM	Data	SM	Data	SM
Four Jets Broad	126	133	19	22	57	57	61	60	23	29	286	299
Many Jets	10	10	1	1.6	6	4.4	8	4.2	3	2.0	28	22
Many Jets + Leptons	22	17	3	2.9	8	7.0	10	7.8	9	3.8	52	39
Four Jets + 2 Leptons	6	4.0	1	0.98	0	2.2	5	2.5	2	1.2	14	11
Many Jets + 2 leptons	6	6.5	2	1.4	2	2.8	2	4.0	3	1.9	15	17
Four Jets+ \cancel{E}	68	77	15	14	35	34	40	37	20	18	178	175
Many Jets+ \cancel{E}	87	80	17	14	50	34	38	36	18	17	210	179

states depending on the W^* decay, they range from ten hadronic jets to six jets associated with leptons and missing energy. The “Many Jets”, “Four Jets” and “Many Jets + Lepton” selections are used to cover these topologies.

Interpreting these results in the framework of the MSSM, Fig. 4(c) shows the 95% C.L. exclusion in the (μ, M_2) plane. As for the $LL\bar{E}$ and $LQ\bar{D}$ couplings the lower limit on the lightest chargino mass is essentially at the kinematic limit.

The searches for the lightest and second lightest neutralino do not extend the excluded region in the (μ, M_2) plane beyond that achieved with the chargino search alone.

6.2 Squarks decaying via $\bar{U}\bar{D}\bar{D}$

The direct decay of pair produced squarks leads to four-quark final states. The “Four Jet” selection is therefore used to extract the mass limits. As shown in Fig. 10(b) the mass limits are 82 GeV/ c^2 for up-type squarks and 68 GeV/ c^2 for down-type squarks.

For the indirect squark decays, which lead to eight-jet topologies, the “Four Jets-Broad” selection is used. The resulting 95% C.L. exclusion in the $(M_{\tilde{\chi}}, M_{\tilde{q}})$ plane for left-handed stop and sbottom are shown in Fig. 13. The corresponding mass limits are $M_{\tilde{t}_L} > 71.5$ GeV/ c^2 and $M_{\tilde{b}_L} > 71.5$ GeV/ c^2 .

6.3 Sleptons decaying via $\bar{U}\bar{D}\bar{D}$

No direct slepton decays are possible via the $\bar{U}\bar{D}\bar{D}$ coupling. For the indirect decays of selectron and smuon pairs, which lead to six-jets plus two-lepton final states, the “Four Jets + 2 Leptons” selection is used for large mass differences between the slepton and neutralino, and the “Many Jets + 2 Leptons” for the low mass difference region. In addition, for the very low mass difference region the leptons are very soft and the “Four Jets” selection is used.

Figure 14 shows the 95% C.L. exclusion in the $(M_\chi, M_{\tilde{\ell}})$ plane for selectrons and smuons. The selectron cross section is evaluated at $\mu = -200 \text{ GeV}/c^2$ and $\tan\beta = 2$. The shape of the limits at $M_\chi \approx 20 \text{ GeV}/c^2$ is due to the switch between selections. For $M_{\tilde{\ell}} - M_\chi > 10 \text{ GeV}/c^2$ this yields $M_{\tilde{e}_R} > 88.5 \text{ GeV}/c^2$ and $M_{\tilde{\mu}_R} > 82.5 \text{ GeV}/c^2$.

6.4 Sneutrinos decaying via $\bar{U}\bar{D}\bar{D}$

No direct sneutrino decays are possible via the $\bar{U}\bar{D}\bar{D}$ coupling. Sneutrinos decaying indirectly lead to six-jet final states containing two neutrinos. Large mass differences between the sneutrino and neutralino lead to event topologies with significant missing energy, and the “Four Jets + \cancel{E} ” selection is used. For small mass differences the “Many Jets + \cancel{E} ” selection is used.

Figure 15 shows the 95% C.L. exclusion in the $(M_\chi, M_{\tilde{\nu}})$ plane for the electron sneutrino (Fig. 15(a)) and muon or tau sneutrino (Fig. 15(b)). The electron sneutrino cross sections is evaluated at $\mu = -200 \text{ GeV}/c^2$ and $\tan\beta = 2$. The limits $M_{\tilde{\nu}_e} > 84 \text{ GeV}/c^2$ and $M_{\tilde{\nu}_{\mu,\tau}} > 64 \text{ GeV}/c^2$ are obtained.

7 Summary

A number of searches were developed to select R-parity violating decay topologies for single and pair production of SUSY particles. It has been assumed that the LSP has a negligible lifetime, and that only one coupling $\lambda_{ijk}, \lambda'_{ijk}$ or λ''_{ijk} is nonzero. These searches found no evidence for R-parity violating supersymmetry in the data collected at $\sqrt{s} = 188.6\text{--}201.6 \text{ GeV}$, and various limits were set within the framework of the MSSM.

From searches for singly produced sneutrinos, upper limits on the values of the λ_{121} and λ_{131} couplings were set as a function of $M_{\tilde{\nu}_\mu}$ and $M_{\tilde{\nu}_\tau}$, respectively.

The limits for direct decays of sleptons for an $LL\bar{E}$ coupling are $M_{\tilde{e}_R} > 92 \text{ GeV}/c^2$ and $M_{\tilde{\nu}_e} > 98 \text{ GeV}/c^2$ at $\mu = -200 \text{ GeV}/c^2$ and $\tan\beta = 2$, $M_{\tilde{\mu}_R, \tilde{\tau}_R} > 81 \text{ GeV}/c^2$ and $M_{\tilde{\nu}_{\mu,\tau}} > 86 \text{ GeV}/c^2$. The limits for the direct decays of sleptons and squarks in the case of an $LQ\bar{D}$ coupling are $M_{\tilde{\mu}_L} > 79 \text{ GeV}/c^2$, $M_{\tilde{\nu}_\mu} > 77 \text{ GeV}/c^2$ and $M_{\tilde{t}_L} > 93 \text{ GeV}/c^2$ for $\text{Br}(\tilde{t}_L \rightarrow q\tau) = 1$. The limit for squarks assuming a $\bar{U}\bar{D}\bar{D}$ coupling are $M_{\tilde{u}_R} > 82 \text{ GeV}/c^2$ and $M_{\tilde{d}_R} > 68 \text{ GeV}/c^2$.

Table 9: The 95% confidence level lower mass limits for sparticles decaying indirectly for each of the three R-parity violating couplings.

Sparticle	Lower mass limit (GeV/ c^2)		
	$LL\bar{E}$	$LQ\bar{D}$	$\bar{U}\bar{D}\bar{D}$
\tilde{t}_1	90	84	71.5
\tilde{b}_1	89	74	71.5
\tilde{e}_R	93	89	88.5
$\tilde{\mu}_R$	92	86	82.5
$\tilde{\tau}_R$	91	73	\times
$\tilde{\nu}_e$	94	89	84
$\tilde{\nu}_{\mu,\tau}$	83	75	64

For the indirect decays of sfermions, the limits listed in Table 9 have been obtained, assuming $M_{\tilde{\ell}} - M_{\chi} > 10$ GeV/ c^2 for $LQ\bar{D}$ and $\bar{U}\bar{D}\bar{D}$, $M_{\chi} > 23$ GeV/ c^2 for $LL\bar{E}$ and derived at $\mu = -200$ GeV/ c^2 and $\tan\beta = 2$ for \tilde{e} and $\tilde{\nu}_e$.

Assuming large m_0 the chargino mass limit is given by the kinematic limit $M_{\chi^+} > 100$ GeV/ c^2 , irrespective of the R-parity violating operator.

8 Acknowledgements

It is a pleasure to congratulate our colleagues from the accelerator divisions for the successful operation of LEP at high energy. We would like to express our gratitude to the engineers and support people at our home institutes without whose dedicated help this work would not have been possible. Those of us from non-member states wish to thank CERN for its hospitality and support.

References

- [1] For a review see for example H.P. Nilles, Phys. Rep. **110** (1984) 1; H. E. Haber and G. L. Kane, Phys. Rep. **117** (1985) 75.
- [2] G. Farrar and P. Fayet, Phys. Lett. **B 76** (1978) 575.
- [3] S. Weinberg, Phys. Rev. **D 26** (1982) 287; N. Sakai and T. Yanagida Nucl. Phys. **B 197** (1982) 83; S. Dimopoulos, S. Raby and F. Wilczek, Phys. Lett. **B 212** (1982) 133.

- [4] ALEPH Collaboration, “*Search for R-parity violating decays of supersymmetric particles in e^+e^- collisions at centre-of-mass energies near 183 GeV*”, Eur. Phys. J. **C13** (2000) 29.
- [5] DELPHI Collaboration, “*Search for supersymmetry with R-parity violating $LL\bar{E}$ couplings at $\sqrt{s} = 183$ GeV*”, Eur. Phys. J. **C13** (2000) 591.
- [6] OPAL Collaboration, “*Searches for R-Parity violating decays of Gauginos at 183 GeV at LEP*”, Eur. Phys. J. **C11** (1999) 619.
- [7] OPAL Collaboration, “*Search for R-parity Violating Decays of Scalar Fermions at LEP*”, Eur. Phys. J. **C12** (2000) 1.
- [8] L3 Collaboration, “*Search for R-Parity Breaking Sneutrino Exchange at LEP*”, Phys. Lett. **B 414** (1997) 373.
- [9] L3 Collaboration, “*Search for R-parity Violating Chargino and Neutralino Decays in e^+e^- Collisions up to $\sqrt{s} = 183$ GeV*”, Phys. Lett. **B 459** (1999) 354.
- [10] ALEPH Collaboration, “*ALEPH: a detector for electron-positron annihilations at LEP*”, Nucl. Instr. Meth. **A 294** (1990) 121.
- [11] ALEPH Collaboration, “*Performance of the ALEPH detector at LEP*”, Nucl. Instr. Meth. **A 360** (1995) 481.
- [12] S. Katsanevas and P. Morawitz, Comp. Phys. Comm. **112** (1998) 227.
- [13] T. Sjöstrand, Comp. Phys. Comm. **82** (1994) 74.
- [14] M. Skrzypek, S. Jadach, W. Placzek and Z. Wąs, Comp. Phys. Comm. **94** (1996) 216.
- [15] *Reports of the working groups on precision calculations for LEP2 Physics*, CERN 2000-009.
- [16] H. Anlauf et al., Comp. Phys. Comm. **79** (1994) 466.
- [17] S. Jadach and Z. Wąs, Comp. Phys. Comm. **36** (1985) 191.
- [18] J.A.M. Vermaseren in “*Proceedings of the IVth international Workshop on Gamma Gamma Interactions*”, Eds. G. Cochar and P. Kessler, Springer Verlag, 1980.
- [19] C. Caso et al., Particle Data Group, Eur. Phys. J. **C3** (1998) 1.
- [20] ALEPH Collaboration, “*Search for supersymmetry with a dominant R-Parity violating $LL\bar{E}$ coupling in e^+e^- collisions at centre-of-mass energies of 130 GeV to 172 GeV*”, Eur. Phys. J. **C4** (1998) 433.

- [21] S. Dimopoulos and L.J. Hall, Phys. Lett. **B 207** (1988) 210; V. Barger, G. F. Giudice and T. Han, Phys. Rev. **D40** (1989) 2987;
H. Dreiner, S. Lola, published in “*Munich/Annecy/Hamburg 1991, Proceedings, e^+e^- collisions at 500 GeV*”; separately in “*Searches for New Physics*”, contribution to the LEP2 workshop, 1996, hep-ph/9602207; and “*Physics with e^+e^- Linear Colliders*”, DESY-97-100, hep-ph/9705442.
- [22] ALEPH Collaboration, *Study of Fermion pair production in e^+e^- collisions at 130-183 GeV* Euro. Phys. J. **C12** (2000) 183.
- [23] B.C. Allanach, A. Dedes and H.K. Dreiner, Phys. Rev. **D 60** (1999) 075014; G. Bhattacharyya, Nucl. Phys. Proc. Suppl. **52A** (1997) 83.
- [24] ALEPH Collaboration, “*Search for charginos and neutralinos in e^+e^- collisions at centre-of-mass energies near 183 GeV and constraints on the MSSM parameter space*”, Euro. Phys. J. **C 11** (1999) 193.
- [25] ALEPH Collaboration, “*Search for supersymmetry with a dominant R-Parity violating $LQ\bar{D}$ coupling in e^+e^- collisions at centre-of-mass energies of 130 GeV to 172 GeV*”, Eur. Phys. J. **C7** (1999) 383.
- [26] D0 Collaboration, “*Search for second generation leptoquark pairs in $p\bar{p}$ collisions at $\sqrt{s} = 1.8$ TeV*”, Phys. Rev. Lett. **84** (2000) 2088;
CDF Collaboration, “*Search for second generation Leptoquarks in the dimuon plus dijet channel of $p\bar{p}$ collisions at $\sqrt{s} = 1.8$ TeV*”, Phys. Rev. Lett. **81** (1998) 4086;
D0 Collaboration, “*Search for first generation scalar leptoquark pairs in $p\bar{p}$ collisions at $\sqrt{s} = 1.8$ TeV*”, Phys. Rev. Lett. **80** (1998) 2051;
CDF Collaboration, “*Search for first generation Leptoquark pair production in $p\bar{p}$ collisions at $\sqrt{s} = 1.8$ TeV*”, Phys. Rev. Lett. **79** (1997) 4327.

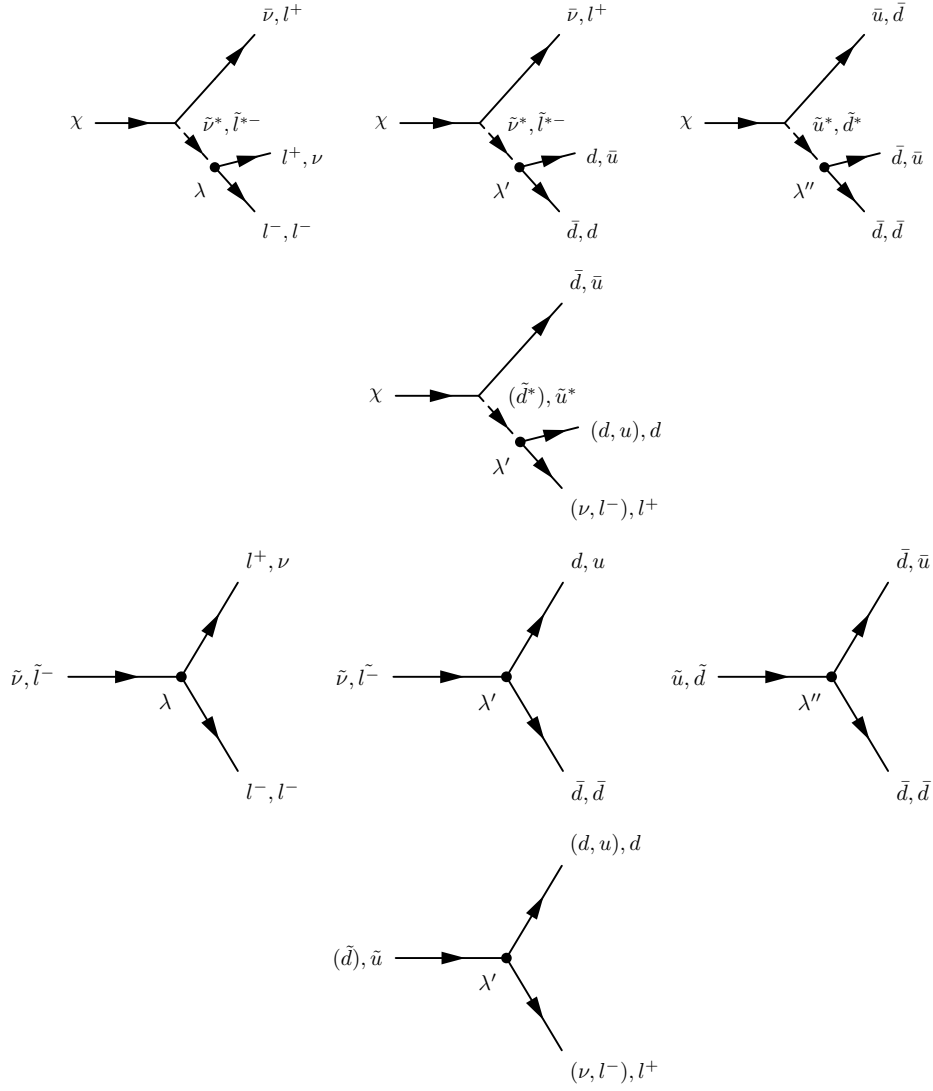


Figure 1: *Direct* R-parity violating decays of supersymmetric particles via the λ , λ' and λ'' couplings. The points mark the R-parity violating vertex in the decay.

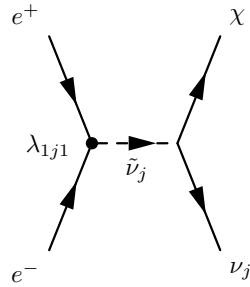


Figure 2: Single sneutrino production via the λ_{1j1} coupling and subsequent *indirect* decay.

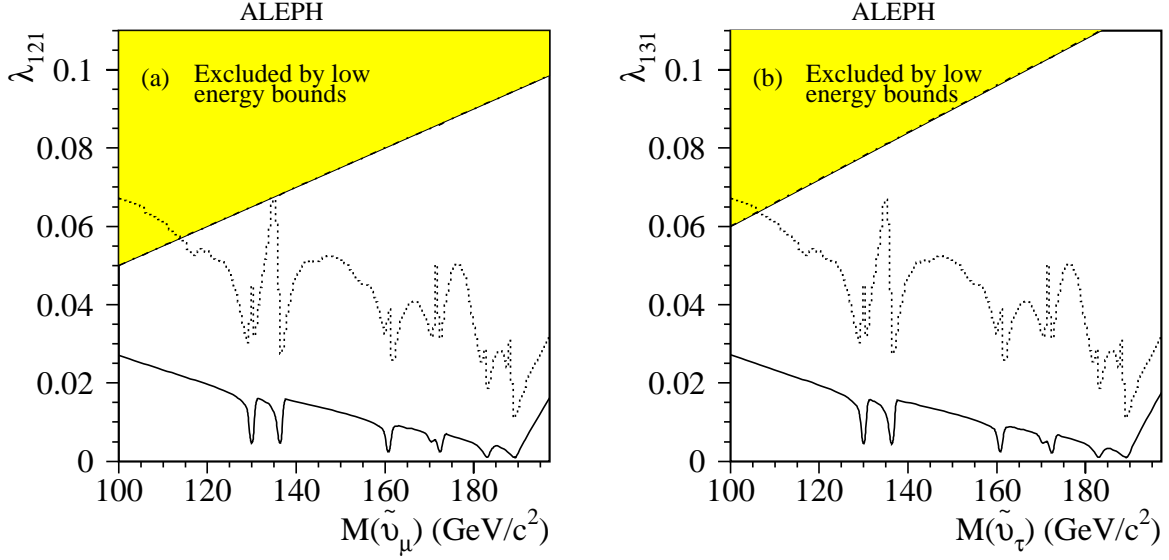


Figure 3: Plots (a) and (b) show the 95% C.L. upper limits on the value of the R-parity violating couplings, λ_{121} and λ_{131} , as a function of sneutrino mass for single sneutrino production and indirect decays (solid curve); the limits are shown for the neutralino mass giving the worst limit. For comparison the limit, assuming 100% branching ratio, for the direct decays to e^+e^- is also shown (dotted histogram). Assuming that $M(\tilde{\nu}_j) = M(\tilde{e}_R)$, the shaded region is excluded by (a) charged current universality and (b) R_τ . The exclusions are evaluated at $\mu = -200 \text{ GeV}/c^2$ and $\tan \beta = 2$.

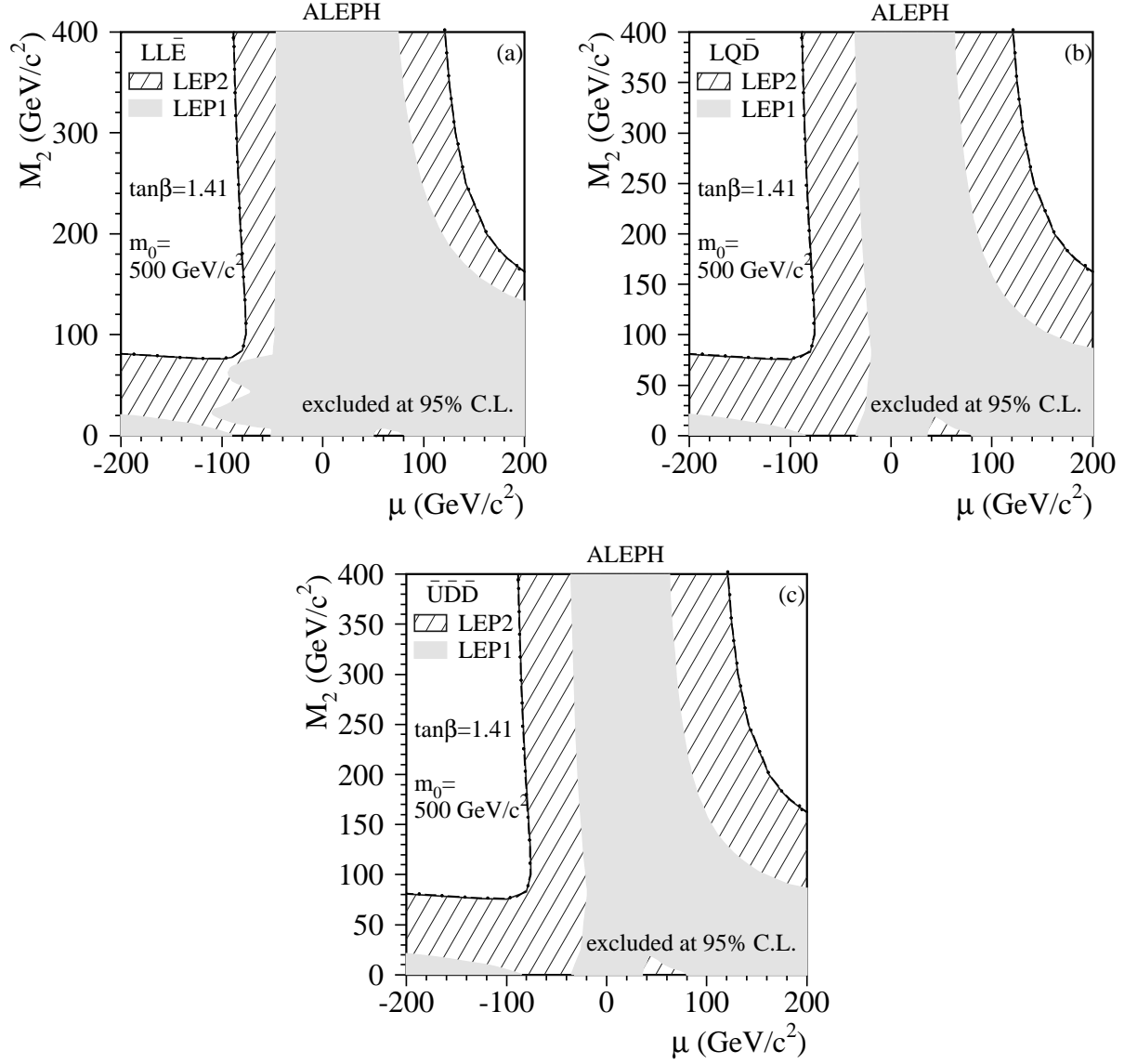


Figure 4: Regions in the (μ, M_2) plane excluded at 95% C.L. at $\tan\beta = 1.41$ and $m_0 = 500 \text{ GeV}/c^2$ for the three operators.

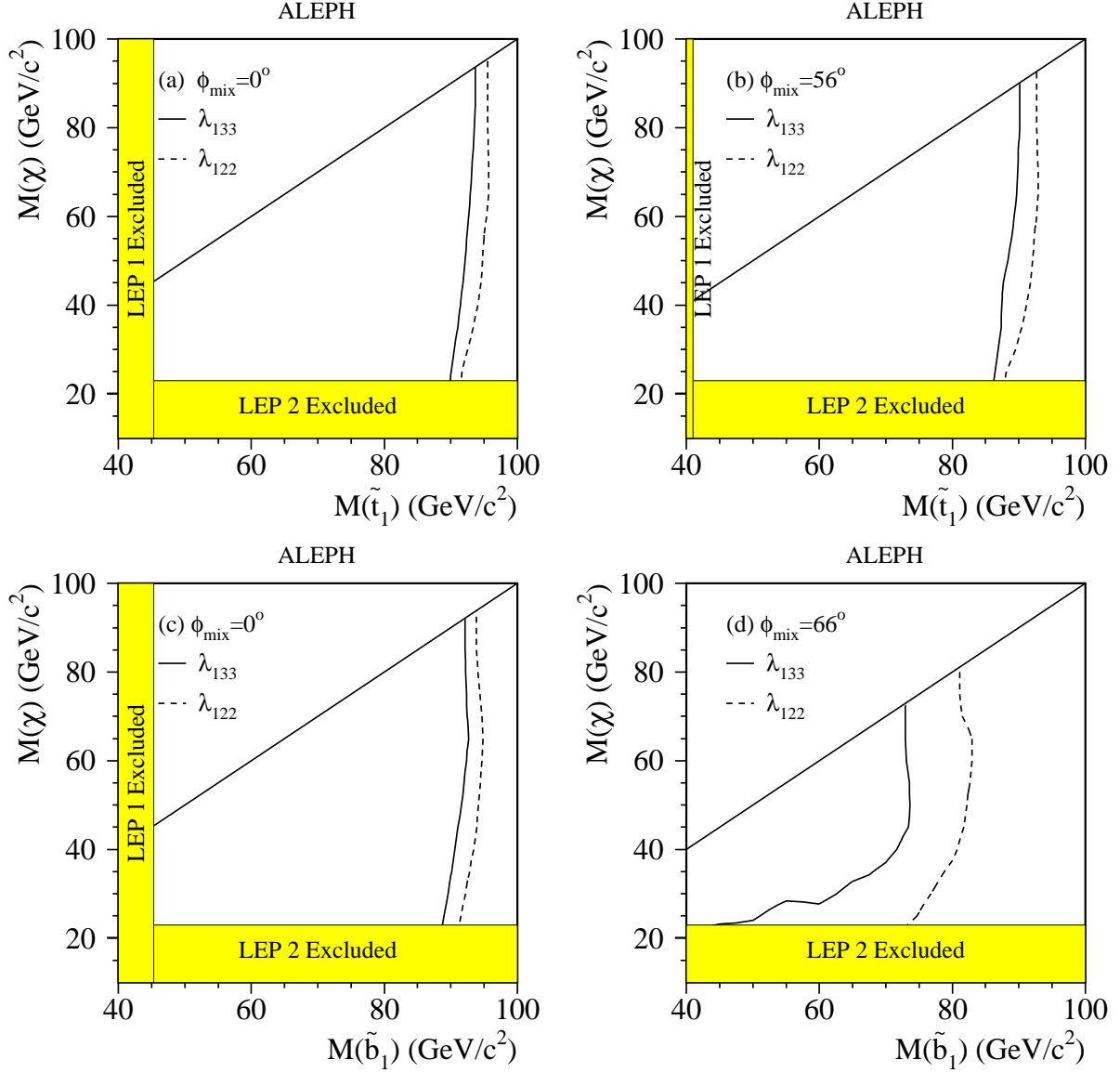


Figure 5: The 95% C.L. limits in the $(M_\chi, M_{\tilde{t}_1})$ and $(M_\chi, M_{\tilde{b}_1})$ planes for indirect decays via the $LL\bar{E}$ couplings λ_{122} and λ_{133} are shown for no mixing ($\phi_{\text{mix}} = 0^\circ$) and for $\phi_{\text{mix}} = 56^\circ, 66^\circ$ for stops and sbottoms, respectively. The LEP 2 exclusion corresponds to the absolute limit on M_χ .

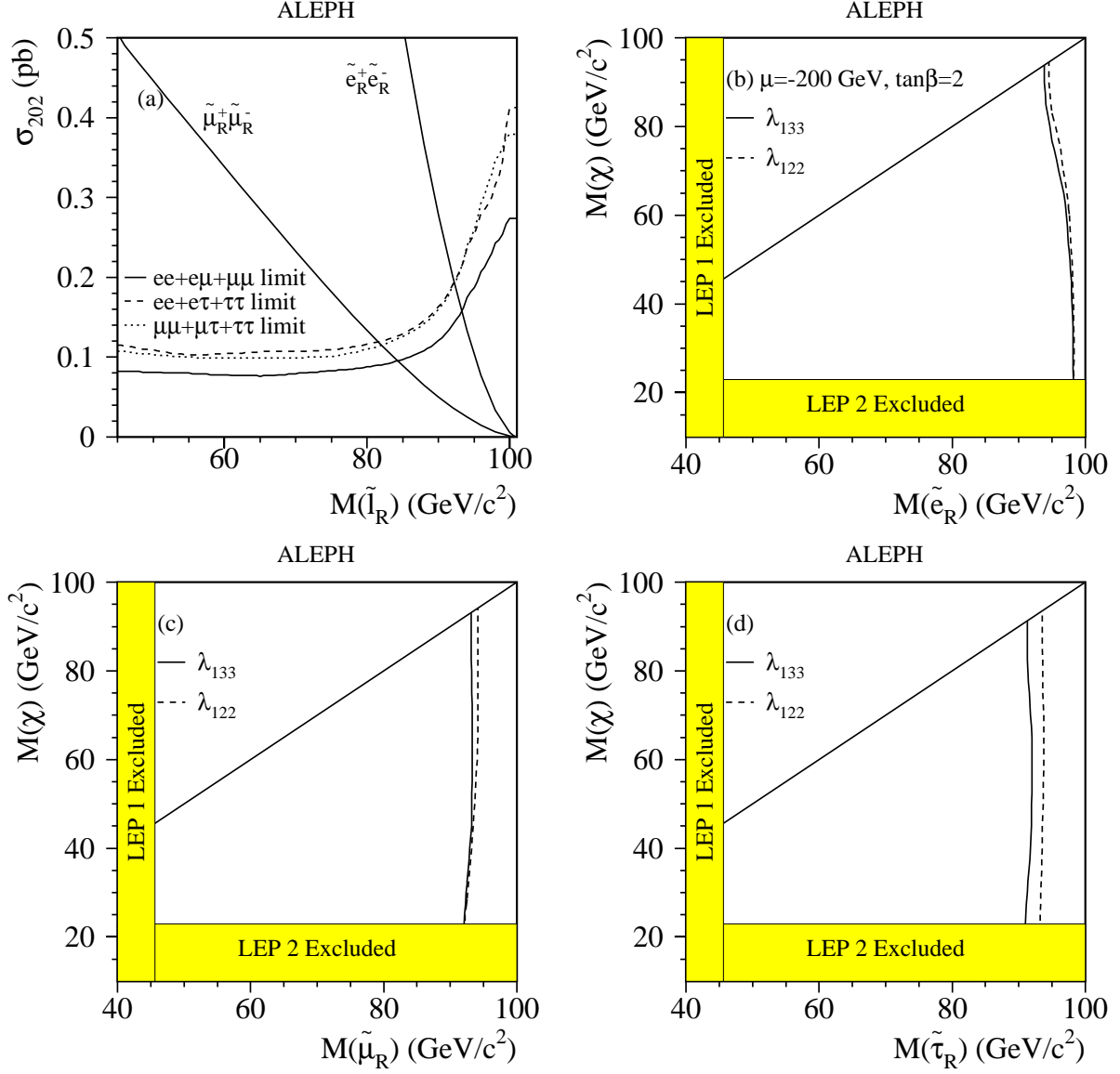


Figure 6: a) The 95% C.L. exclusion cross sections for sleptons decaying directly via a dominant $LL\bar{E}$ operator. The MSSM cross section for pair production of right-handed selectrons and smuons are superimposed. Figures b), c) and d) show the 95% C.L. limits in the $(M_\chi, M_{\tilde{l}_R})$ plane for indirect decays of selectrons, smuons and staus, respectively. The two choices of λ_{122} and λ_{133} correspond to the best and worst case exclusions, respectively. The selectron cross section is evaluated at $\mu = -200$ GeV/c² and $\tan\beta = 2$.

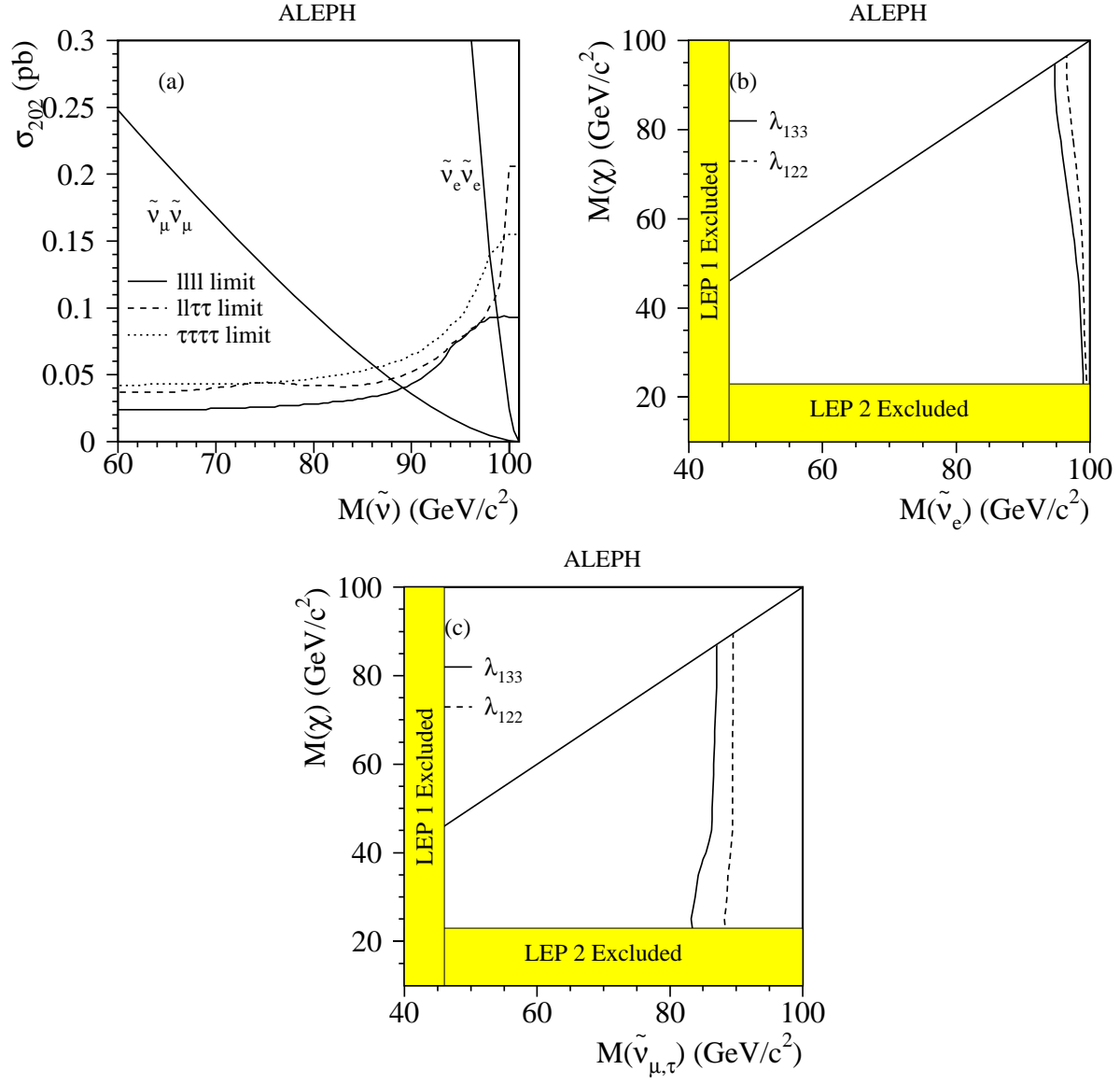


Figure 7: (a) The 95% C.L. exclusion cross sections for sneutrinos decaying directly via a dominant $LL\bar{E}$ operator. The MSSM cross section for pair production of muon and electron sneutrinos are superimposed; the tau sneutrinos have the same cross section as the muon type. Figure (b) shows the 95% C.L. limits in the $(M_\chi, M_{\tilde{\nu}})$ plane for $\tilde{\nu}_e$, and figure (c) for both $\tilde{\nu}_\mu$ and $\tilde{\nu}_\tau$ indirect decays. The two choices of λ_{122} and λ_{133} correspond to the best and worst case exclusions, respectively. The electron sneutrino cross section is evaluated at $\mu = -200$ GeV/c² and $\tan\beta = 2$.

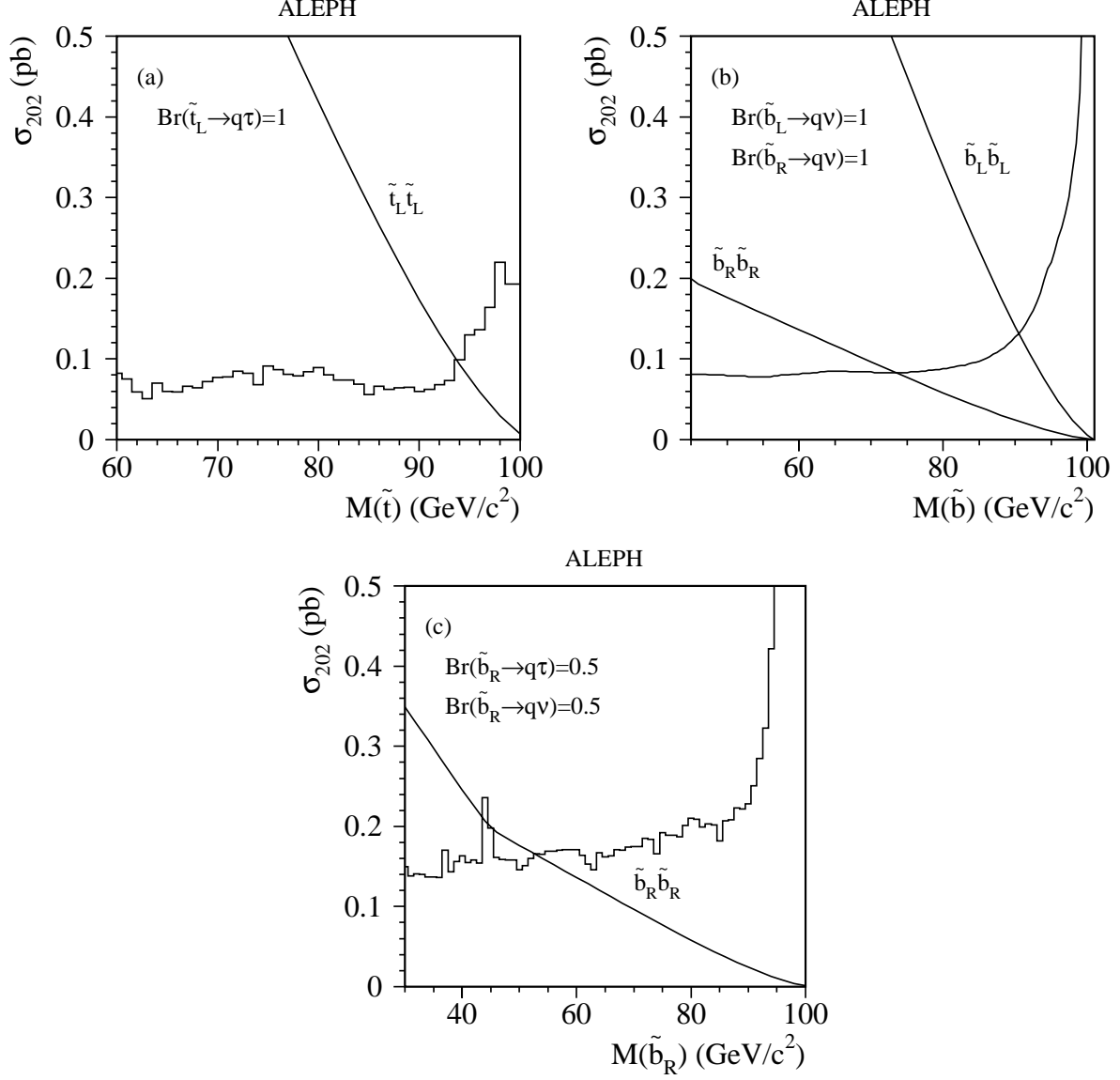


Figure 8: The 95% C.L. excluded cross sections for the production of squarks decaying directly via a dominant $LQ\bar{D}$ operator: (a) \tilde{t}_L (λ'_{33k}), (b) \tilde{b}_L (λ'_{i3k}) or \tilde{b}_R (λ'_{i33}), and (c) \tilde{b}_R (λ'_{3j3}). The MSSM cross sections are superimposed.

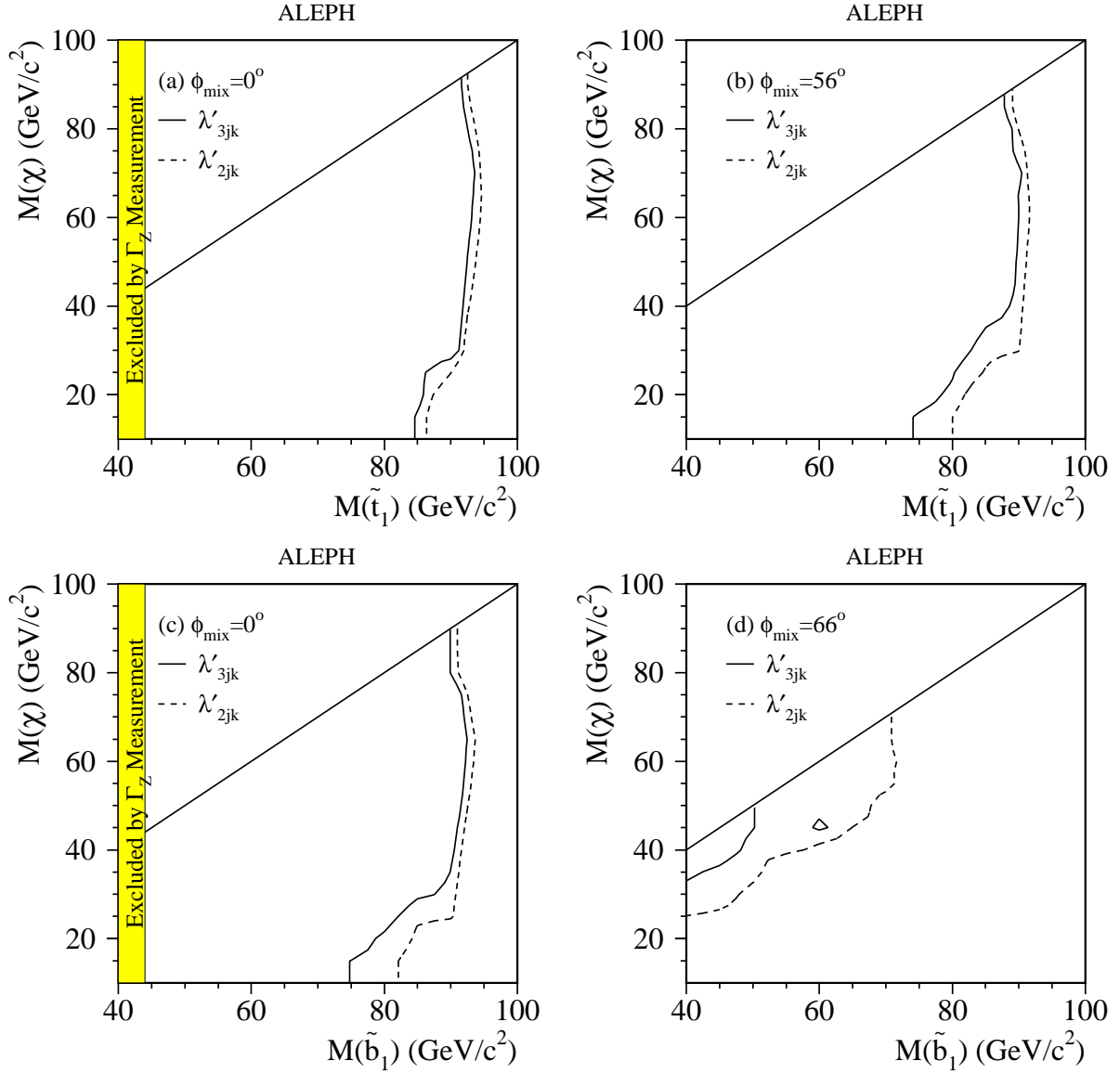


Figure 9: The 95% C.L. limits in the $(M_\chi, M_{\tilde{t}_1})$ and $(M_\chi, M_{\tilde{b}_1})$ planes for indirect $LQ\bar{D}$ decays via the λ'_{211} and λ'_{311} couplings, for no squark mixing ($\phi_{\text{mix}} = 0^\circ$) and for $\phi_{\text{mix}} = 56^\circ, 66^\circ$ for stops and sbottoms, respectively.

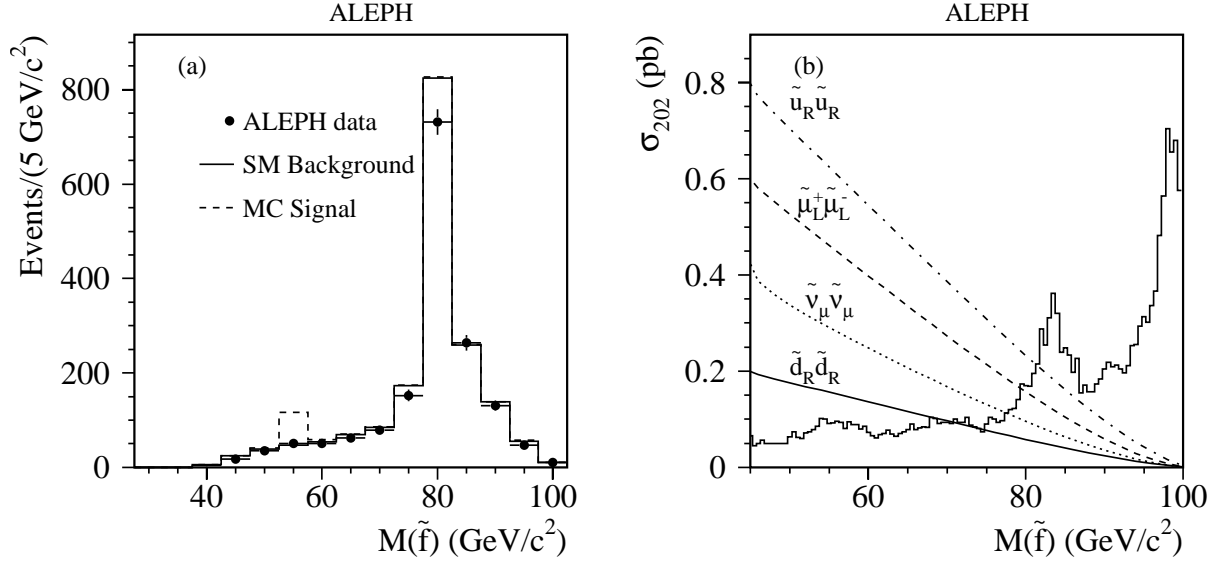


Figure 10: (a): The distribution of the reconstructed invariant masses for jet pairs after forcing the event into four jets. The points are the data (from 188.6 GeV to 201.6 GeV), the solid histogram is the Monte Carlo predicted background. The dashed histogram is the signal for the process $e^+e^- \rightarrow \tilde{\mu}_L^+ \tilde{\mu}_L^-$ with the smuons decaying directly via the $LQ\bar{D}$ coupling; here $M_{\tilde{\mu}_L} = 55 \text{ GeV}/c^2$ and the histogram is normalised to the expected cross section for this process ($\sigma = 0.46 \text{ pb}$ at $\sqrt{s} = 202 \text{ GeV}$). (b): The 95% C.L. excluded cross sections for sleptons (via $LQ\bar{D}$), sneutrinos (via $LQ\bar{D}$) and squarks (via $\bar{U}\bar{D}\bar{D}$) decaying directly to four jets. The MSSM cross sections for pair production of muon sneutrinos, left-handed smuons and right-handed squarks are superimposed.

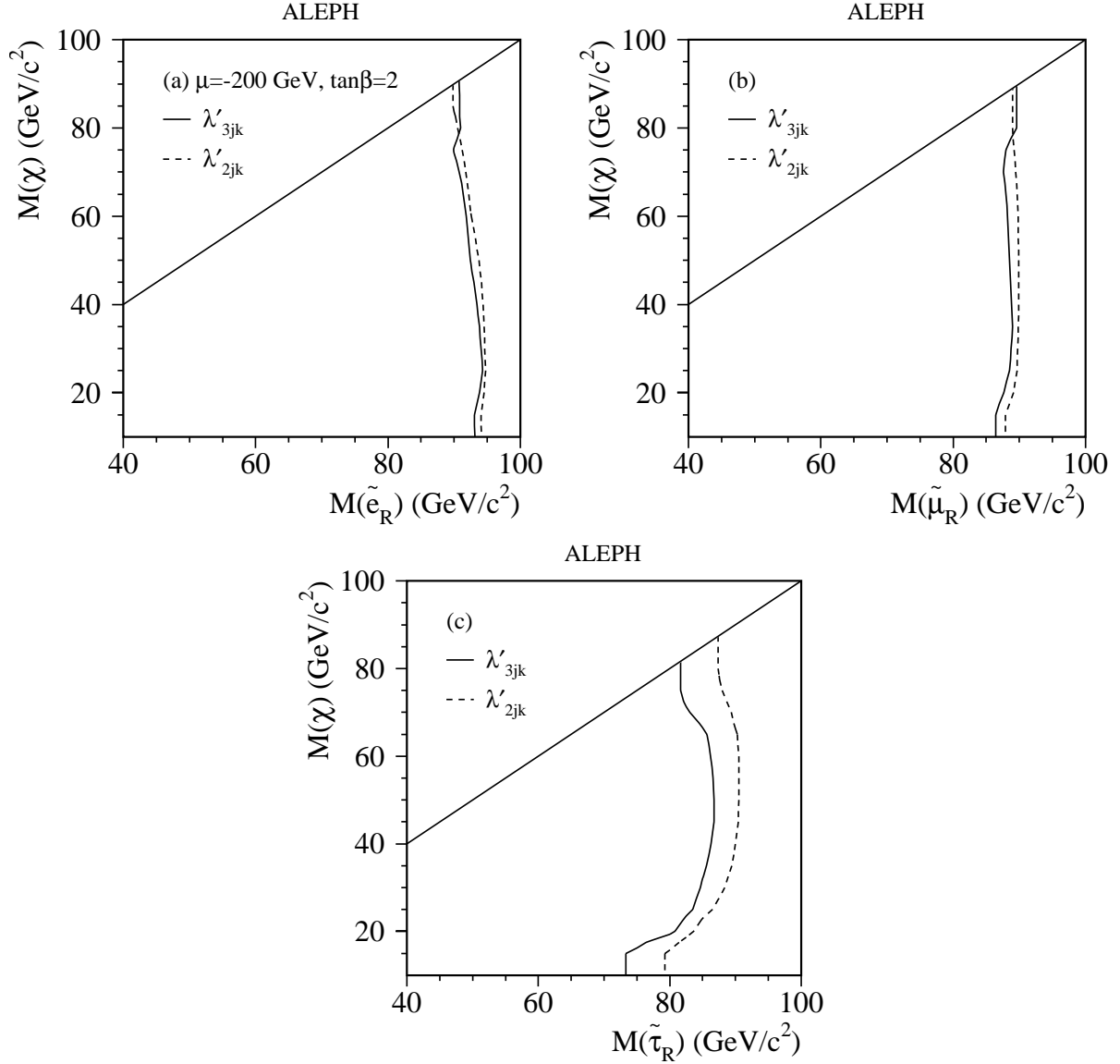


Figure 11: The 95% C.L. limits in the $(M_\chi, M_{\tilde{l}_R})$ plane for selectrons, smuons and staus decaying indirectly via a dominant $LQ\bar{D}$ operator. The two choices of λ'_{2jk} and λ'_{3jk} correspond to the best and worst case exclusions, respectively. The selectron cross section is evaluated at $\mu = -200$ GeV/c² and $\tan\beta = 2$. The limit from the Γ_Z measurements excludes $M_{\tilde{l}} < 38$ GeV/c².

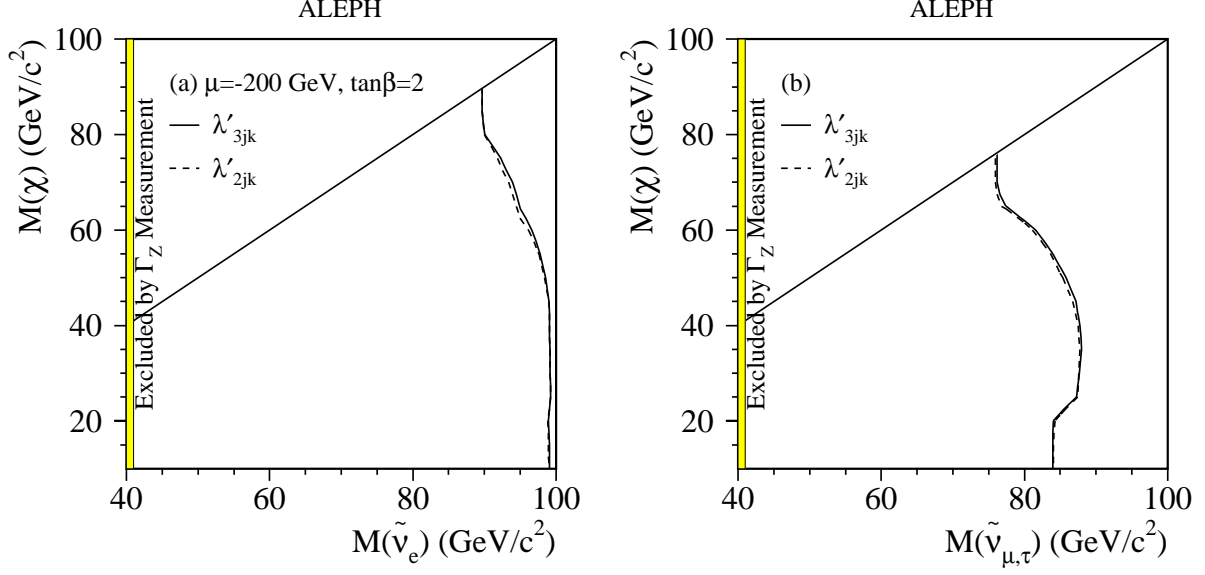


Figure 12: The 95% C.L. limits in the $(M_\chi, M_{\tilde{\nu}})$ plane for electron and muon or tau sneutrinos decaying indirectly via a dominant $LQ\bar{D}$ operator. The two choices of λ'_{2jk} and λ'_{3jk} correspond to the best and worst case exclusions, respectively. The electron sneutrino cross section is evaluated at $\mu = -200 \text{ GeV}/c^2$ and $\tan \beta = 2$.

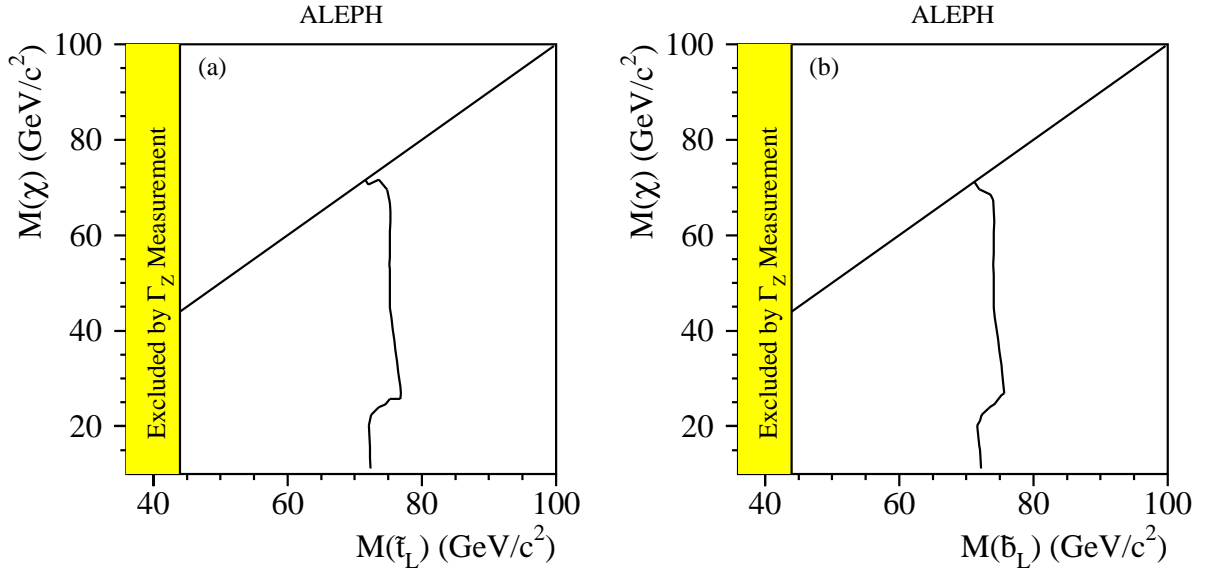


Figure 13: The 95% C.L. exclusion in the $(M_\chi, M_{\tilde{q}})$ plane for a) left-handed stop, b) left-handed sbottom decaying indirectly via a dominant $\bar{U}\bar{D}\bar{D}$ operator.

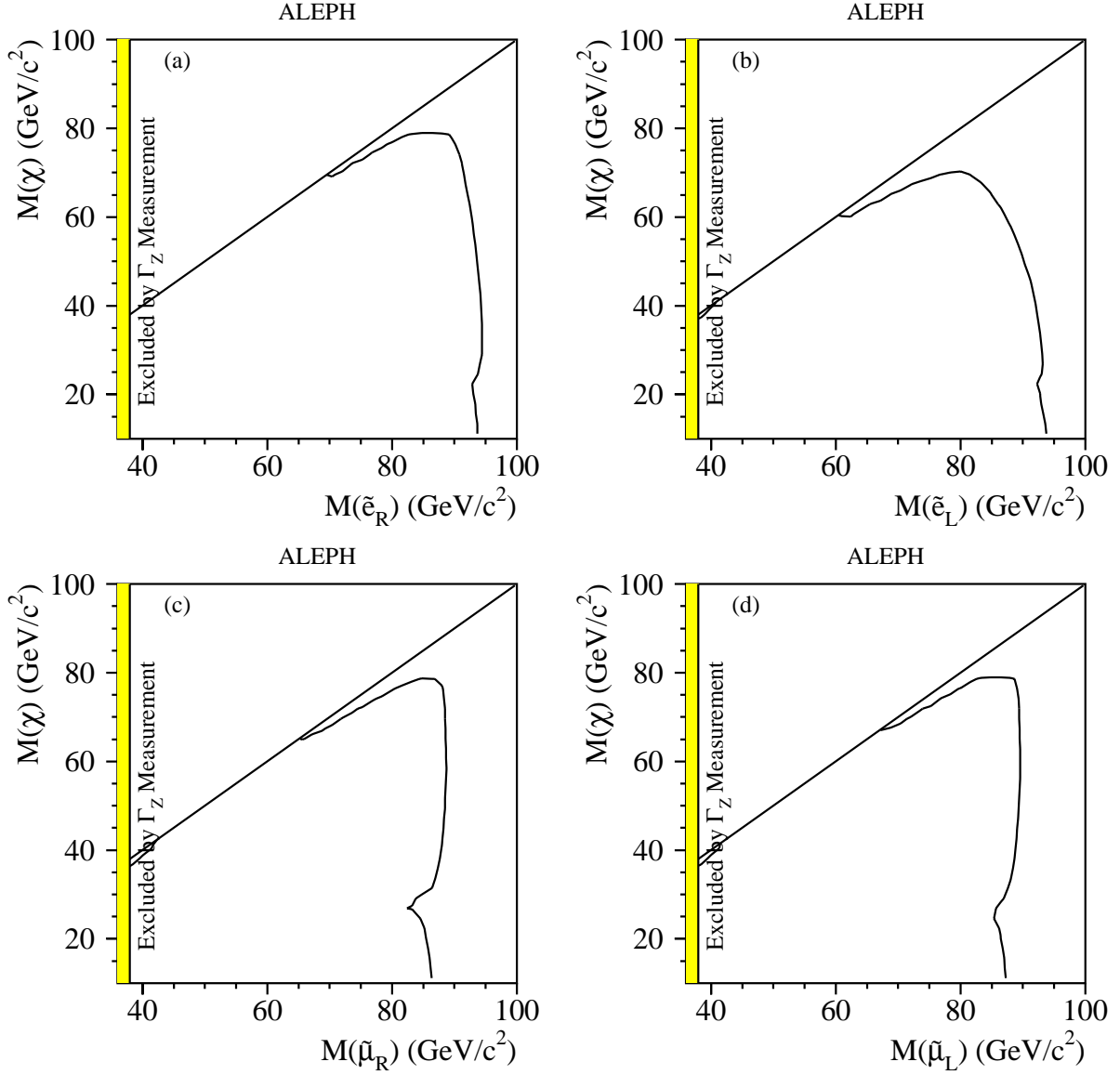


Figure 14: The 95% C.L. excluded cross sections for left or right-handed selectrons and smuons decaying indirectly via a dominant $\bar{U}\bar{D}\bar{D}$ operator. The selectron cross section is evaluated in the region $\mu = -200$ GeV/c² and $\tan\beta = 2$.

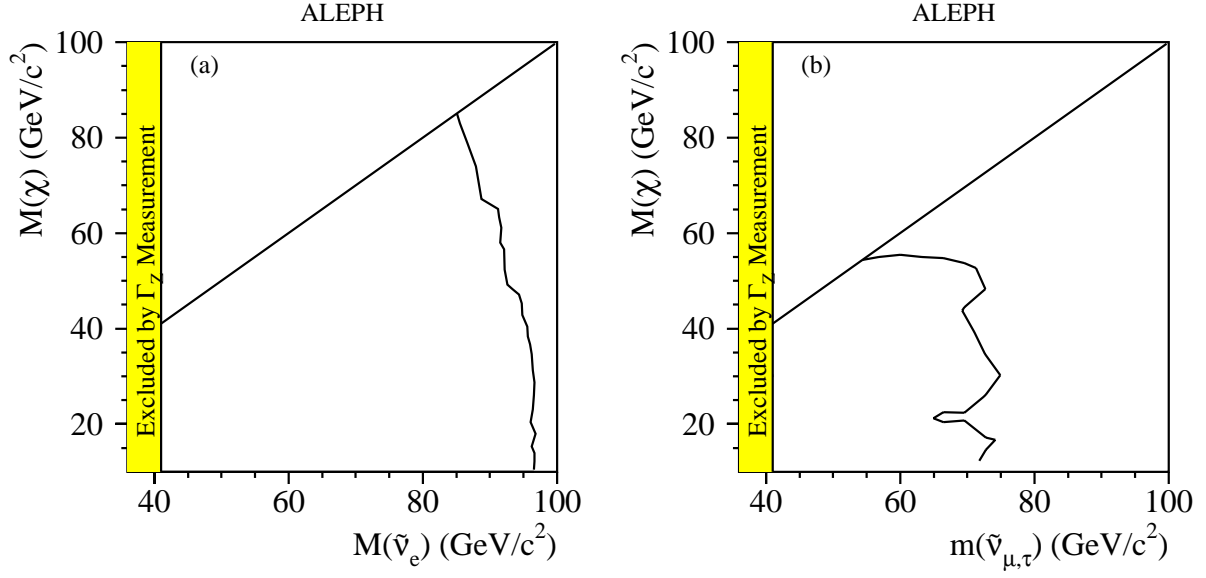


Figure 15: (a) The 95% C.L. exclusion in the $(M_\chi, M_{\tilde{\nu}})$ plane for $\tilde{\nu}_e$ decaying indirectly via a dominant $\bar{U}\bar{D}\bar{D}$ operator. The $\tilde{\nu}_e$ cross section is evaluated at $\mu = -200$ GeV/c² and $\tan\beta = 2$. (b) The exclusion obtained in the $(M_\chi, M_{\tilde{\nu}_{\mu,\tau}})$ plane for $\tilde{\nu}_{\mu,\tau}$ decaying indirectly via a dominant $\bar{U}\bar{D}\bar{D}$ operator.